Master of Science Thesis in Electrical Engineering
Department of Electrical Engineering, Linköping University, 2022

Effects of Dynamic Modeling on the Path Planning of Simulated Autonomous Vehicles

Elin Kidell Löwstedt

LINKÖPING UNIVERSITY

Master of Science Thesis in Electrical Engineering

Effects of Dynamic Modeling on the Path Planning of Simulated Autonomous Vehicles

Elin Kidell Löwstedt

LiTH-ISY-EX–22/5530—SE

Supervisor: **Björn Olofsson**
ISY, Linköpings universitet
Aghyad Jabali
Syntronic Research and Development, Linköping

Examiner: **Jan Åslund**
ISY, Linköpings universitet

Division of Vehicular Systems
Department of Electrical Engineering
Linköping University
SE-581 83 Linköping, Sweden

Abstract

The purpose of the thesis was to evaluate the robustness of the Hybrid A* algorithm in regards to the levels of dynamic vehicle modeling, vehicle parameters and driving velocity. The original scope of the thesis project was to alter vehicle and tire models but this was discovered to be out of the time limits of the thesis project. The new scope was to alter the parameters with close connection to the vehicle dynamics, such as tire friction, vehicle mass and driving velocity. The thesis project was performed in collaboration with Syntronic and their internal project Autodrive.

Due to the complexity of the system, tests were first performed to evaluate if the path planner and path following were deterministic. Variation of tire friction, vehicle mass, reference velocity and maximum steering was then performed during three different driving missions designed to simulate different complexity levels of realistic driving scenarios. The dependence of the varied vehicle parameters on the deterministic behaviour was also examined. Lastly, the impact of altering parameters used for smoothing of the Hybrid A* solution and parameters of the controller were explored and analysed. The position of the vehicle, the velocity profile, slip angles and angular acceleration were used in order to draw conclusions regarding the performance of Hybrid A*, the motion control and the limitations of vehicle and tire models.

The results showed that the implementation used of Hybrid A* is deterministic but fail to produce a consistent route when faced with obstacles and re-planning due to the vehicle control not being deterministic. Variation in vehicle mass and reference velocity as well as the aggressiveness of the course were concluded to impact the determinism of the path following. The best values for the smoothing parameters are dependent on the desired vehicle behaviour, but can be used to reduce the difference between the planned and followed path.

The Hybrid A* planner was concluded to be robust in regards to variations in vehicle mass, tire friction and maximum steering angles but very sensitive to a change in velocity. The slip angles were generally small, but the kinematic single-track model theoretically only hold when the slip angles are zero. The results did, however, indicate that the implementation of the Hybrid A* algorithm was able to produce a drivable and realistic path for all cases except the most extreme parameter choices. For larger velocities and unrealistically low tire friction, the dynamic single-track model is more suitable.

The choice of vehicle model is not critical except when using high driving velocities. It is important to have knowledge of the desired driving velocity when choosing a dynamic model, but the solution of the implemented path planner and path following is otherwise robust enough to handle a less advanced model. The current implementation of the Hybrid A* algorithm, using the kinematic single-track model, can therefore be concluded to be sufficient in planning a realistic path for a simulated autonomous vehicle for low driving velocities, while a more advanced model is needed when increasing the driving velocity.

Acknowledgments

First of all would I like to thank Syntronic for giving me the opportunity of working with this exciting thesis project. It has been interesting, challenging, of course hard at times but mostly very fun and educational. I would like to thank my supervisor Aghyad Jabali but also all other employees for always being helpful and happy to help. An extra big thank you goes out to Mattias Lindgren and Niklas Larsson for supporting and assisting me during this thesis project.

Secondly I would like to thank my supervisor and examiner at Linköping University, Björn Olofsson and Jan Åslund. Thank you for helping me through all the twists and turns of the thesis project with your fantastic support and guidance.

Lastly I would like to thank my partner Albin for your encouragements, support and for always believing in me. I would also like to thank my family and friends who have supported me, I could not have done it without you.

Contents

Notation

Notations

Notation	Meaning
α_f	Slip angle for front wheel, single-track model
α_r	Slip angle for rear wheel,single-track model
β	Vehicle side slip angle
δ_f	Steering angle for front wheel, single-track model
δ_i	Steering angle for outer wheel in curve
δ_o	Steering angle for outer wheel in curve
δ_r	Steering angle for rear wheel, single-track model
ψ	Inertial heading
$\dot{\psi}$	Yaw rate
B	Track width
$C_{\alpha,f}$	Cornering stiffness front tire
$C_{\alpha,r}$	Cornering stiffness rear tire
I_z	Yaw inertia
l_r	Distance between rear wheel and CG
l_f	Distance between front wheel and CG
L	Wheel base
m	Vehicle mass
R	Turning radius
V	Speed of the vehicle
v_x	Longitudinal velocity of the vehicle
v_y	Lateral velocity of the vehicle
v_z	Velocity in upward/downward direction of the vehicle
(x, y)	Body-fixed coordinates
(X, Y)	Inertial coordinates
$\dot{x}$	Longitudinal speed in body coordinates
$\dot{y}$	Lateral speed in body coordinates

Abbreviations

Abbreviation	Meaning
CG	Center of gravity
DM1	Driving mission 1
DM2	Driving mission 2
DM3	Driving mission 3
PID	Proportional, integral, differential (controller)

1 Introduction

The focus of this thesis is to study the Hybrid A* algorithm[1], vehicle dynamics and the effects different vehicle settings, road parameters and driving velocities have on a simulated autonomous vehicle. The simulations of the autonomous vehicle are performed in the simulation environment CARLA [2] and the autonomous vehicle is operated using ROS [3]. This chapter provides an introduction to the project in order to define the problem at hand and provide an understanding of the motivation, background and purpose of the project. A description of other work related to the subject is also presented.

1.1 Motivation and background

The thesis project was performed in collaboration with the company Syntronic. A project at the company is the Autodrive 3 project, which this thesis project is a part of. The Autodrive project is an internal project at Syntronic and is currently under development. The previous two versions, Autodrive 1 and Autodrive 2, are predecessors to this version. Autodrive 3 aims to develop a simulation environment in CARLA with the ability to simulate autonomous vehicles such as cars, trucks and robots using ROS [3] and ROS bridge [4]. In this report, the term Autodrive refers to the current version of the system, if nothing else is implied.

The topic of autonomous driving is currently very relevant and many companies are getting involved in the industry. The Autodrive project is, however, only purposed to be used virtually and there are currently no plans in applying the solutions in a real vehicle. It is instead only used for simulation purposes. Running tests in a virtual environment have many advantages, including controllability, reproducibility and standardization of driving tests. It is also easier to obtain

data and try cases that would, in real life, be a danger to the driver [5].

The thesis project will focus on the path-planning algorithm and analyse the behaviour of the Hybrid A* algorithm and how well the desired path can be followed depending on the chosen vehicle and road parameters as well as driving velocity. This is important in order to achieve realistic simulations for different kinds of vehicles. In the current version of Autodrive, the Hybrid A* algorithm uses a kinematic model based on a single-track vehicle model. The single-track model is a simple approximation of a 4-wheeled vehicle [6]. In order to achieve realistic behaviour in autonomous driving, it is essential to understand how this simplification and the limitations of the Hybrid A* algorithm affect the overall behaviour of the algorithm in different scenarios.

1.2 System description

The main system consists of CARLA, ROS bridge and ROS. The subsystem Autodrive is responsible for handling all functionality of the vehicle and uses ROS as the operating system to control and send information to CARLA. Everything that is altered, computed or discussed about the system in this thesis project relates to the Autodrive system unless anything else is stated. An overview of the system is shown in Figure 1.1.

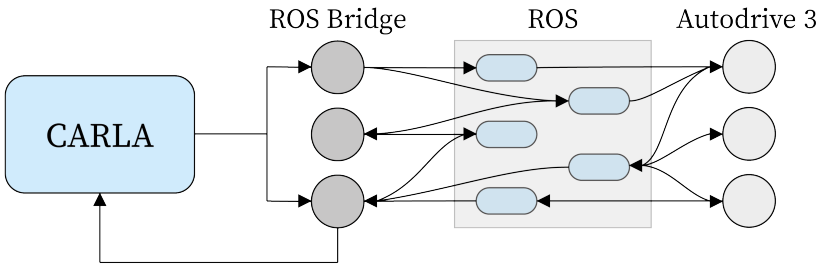

Figure 1.1: *Overview of the system.*

ROS is an open-source robot operating system and uses so called nodes, which are processes that perform different kinds of computations in the system. Nodes communicate with each other by passing messages through ROS topics. A node can subscribe or publish to another node as shown in Figure 1.2 [3]. ROS bridge is a two-way communication between CARLA and ROS and enables information transfer between the two. ROS bridge is responsible for translating information sent between nodes, such as steering commands, to CARLA and obtaining data from CARLA in return. This received information can for example be sensor data from the vehicle [4].

Figure 1.2: *Communication between nodes in ROS.*

Figure 1.3 shows a screenshot of the simulation environment CARLA with the simulated autonomous vehicle present. There are default maps available but it is also possible to create custom maps to represent for example a city, a mine or an industrial area as shown in Figure 1.3.

Figure 1.3: *Vehicle in the simulation environment CARLA.*

1.2.1 Motion planning and control

The Hybrid A* path planner and the motion controller are located in the Autodrive subsystem. These, along with some parts of the CARLA environment, are the most important parts of the thesis project and are the only functions that will be altered and investigated further. A schematic overview of the program responsible for motion planning and control is shown in Figure 1.4 and it consists of the path planner and the vehicle control.

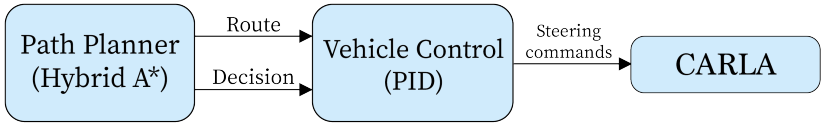

Figure 1.4: *Overview of the motion planning and control.*

The path planner uses a Hybrid A* algorithm, which is implemented according to the paper *Application of Hybrid A* to an Autonomous Mobile Robot for Path Planning in Unstructured Outdoor Environments* [1]. This algorithm uses a single-track model to account for the kinematic constraints on the vehicle. The path planner sends the route and decision to the vehicle control block, which in turn is responsible for following the desired path. The decision indicates which type of state the vehicle is in, for example normal driving or reversing. The vehicle control uses a PID controller for computing the steering commands and for speed control. The steering commands are published to the relevant ROS-topics and are sent to CARLA through the ROS bridge. The steering commands contain the steering angle for each one of the two front wheels.

Currently, the vehicle types supported in Autodrive are 4-wheeled and 2-wheeled vehicles. In case of using the 4-wheeled vehicle, the Hybrid A* algorithm is used to calculate the planned path. If the 2-wheeled vehicle is used, an A* algorithm is used instead. There is also a separate PID-controller for the 2-wheeled and 4-wheeled vehicles, respectively. In this thesis project, only the 4-wheeled vehicle will be used.

The main motivation of the thesis is to investigate if the current system is suitable for describing the vehicle behaviour in realistic driving scenarios or what alterations needs to be made to achieve this goal.

1.3 Problem formulation

The purpose of the Master Thesis is to evaluate and analyse the robustness of the solution given by a path-planning algorithm in regards to vehicle dynamics parameters and velocity, in this particular case a Hybrid A* search algorithm. The goal is to find what level of vehicle modeling is needed in order to sufficiently describe the vehicle behaviour in realistic driving scenarios. In order to achieve this, the following questions need to be answered:

- Which vehicle and tire models are available and suitable in terms of complexity?
- Which assumptions are made for each model and in what cases are these assumptions reasonable to make?
- How do effects caused by high driving velocities affect the solution given by the path-planning algorithm?
- How do different levels of accuracy in terms of vehicle modeling affect the solution given by the path-planning algorithm?

1.4 Delimitations

The focus of this thesis project is to study vehicle dynamics and the effects different vehicle models and velocities have on a simulated autonomous vehicle. In

order to do so, it will be important to understand the path-planning algorithm used in simulation. However, the goal is not to improve the path-planning algorithm itself in order to find the best solution to the shortest-path problem.

1.5 Related work

The field of autonomous driving and the use of Hybrid A* search algorithms have been well studied.

The paper *Application of Hybrid A* to an Autonomous Mobile Robot for Path Planning in Unstructured Outdoor Environments* [1] covers the implementation of the Hybrid A* algorithm using a single-track model. It provides a description of motion primitives and the conditions on driving distance, heading change and steer angle that need to be satisfied. The paper describes the Hybrid A* algorithm in detail as well as extensions to this algorithm, such as methods to plan the route via several waypoints and taking terrain characteristics into consideration.

The papers *Practical Search Techniques in Path Planning for Autonomous Driving* [7] and *Path Planning for Autonomous Vehicles in Unknown Semi-structured Environments* [8] explain the concepts of the Hybrid-State A* algorithm. The algorithm associates a continuous 3D-state of the vehicle to each grid cell in the discretized search space. It is noted that the Hybrid-State A* algorithm is not guaranteed to find the optimal path, but it is guaranteed to be drivable. The algorithm can plan both forward and reverse motion, but the act of driving in reverse and changing direction is penalized. It is described that the search algorithm is guided by two heuristics: the first takes the nonholonomic characteristics of the vehicle into account and the second uses the obstacle map to compute the shortest distance to the goal.

A Survey of Motion Planning and Control Techniques for Self-Driving Urban Vehicles [9] describes planning and control algorithms for self-driving vehicles. It is explained that the decision making of an autonomous vehicle consists of four stages: route planning, behavioural decision making, motion planning and vehicle control. The route planning is responsible for planning the route from start to goal by calculating the most cost-effective way to traverse the map. The behavioural decision decides on appropriate driving behaviour when taking other vehicles, obstacles and rules into account. The motion planning creates a route or trajectory that is dynamically feasible for the vehicle and the vehicle control is responsible for following the desired path with the use of a feedback controller. The kinematic single-track model is used in control and motion planning to model the constraints on the vehicle. The paper discusses some possible approaches for a path-planning algorithm, where Hybrid A* is one of the options.

In *A Simplified Vehicle Dynamics Model for Motion Planner Designed by Nonlinear Model Predictive Control* [10], it is discussed how different vehicle models in terms of complexity affect the solution given by the motion planner using a nonlinear model predictive controller. The models used in the study were a simple kine-

matic single-track model, a dynamic single-track model using the Magic formula tire model (See Section 2.3.3) to approximate the lateral forces on the vehicle and a coupled dynamic model. It was concluded that the error in lateral speed and yaw rate increased with higher velocities for the kinematic model and that a big steering angle decreased the accuracy of the dynamic model. However, the coupled model achieved good accuracy in all these cases.

The paper *Controller Design for Autonomous Vehicle* [11] describes simulations of autonomous vehicles in CARLA using a longitudinal and lateral controller for speed and steering, respectively. A PID controller was used for speed control, controlling the throttle and brakes to achieve the desired speed. A combination of a Stanley controller and feedback proportional control was used for steering control. A single-track model was used to describe the lateral characteristics of the vehicle. It was concluded that this method resulted in accurate following at low speeds. The paper proposed that a sliding mode control or a MPC could be used for the lateral controller when driving at higher speeds in order to take dynamic effects into account.

In the paper *The kinematic single-track model: A consistent model for planning feasible trajectories for autonomous vehicles?* [12], the effects of modeling for both the motion planning and the vehicle control using a kinematic single-track model in comparison with a more complex and realistic vehicle model was evaluated. It was concluded that the kinematic model was consistent in producing a feasible trajectory during the motion planning phase. The authors emphasize the importance of limiting the value of the lateral acceleration while using this model, since the modeling errors increase along with an increasing acceleration.

This thesis project aims to investigate how the simplifications made by the Hybrid A* algorithm when using the kinematic single-track model affect the behaviour when faced with different degrees of realistic driving missions. As described, the kinematic single-track model is usually considered adequate when the conditions are fairly simple and non-extreme and the dynamic single-track model is often deemed good-enough in other cases. It will be examined how factors that are not taken into consideration by the kinematic single-track model or the dynamic single-track model affect the solution, which is not discussed in much detail by other related work. The limitations of the PID controller as both speed and steering control will also be examined.

2
Theory

This chapter describes the theory necessary to form an understanding of the project at hand. Topics such as vehicle models, tire models, path planning algorithms and controller design are covered.

2.1 Simulation environment and ROS

CARLA uses the physics engine Unreal Engine 4[2]. The vehicle dynamics is defined in this engine, and the motion of the vehicle is described through a dynamic vehicle model. The model defines the vehicle motion as

$$\begin{aligned} v_{i+1} &= v_i + \frac{F}{m}\Delta t \\ w_{i+1} &= w_i + \frac{M}{I_z}\Delta t \\ p_{i+1} &= p_i + v\Delta t \end{aligned} \tag{2.1}$$

where v is the velocity, Δt the difference in time between time instant i and i+1, w is the angular velocity, p is the position, F is the force on the chassis, M is the torque and I_z the inertia.

2.2 Vehicle models

This section presents some of the vehicle models that will be relevant to the project and basic definitions related to the topic of vehicle dynamics.

2.2.1 Basic definitions of vehicle dynamics

For a vehicle with wheels, there is an individual side slip angle for each tire and a side slip angle defined for the vehicle as a whole, the latter is also referred to as the vehicle side slip angle. The side slip angles for each tire is defined as the angle between the direction of the tire and the orientation of its velocity vector and the vehicle side slip angle is defined as the angle between the longitudinal axis of the vehicle and the orientation of its velocity vector [13]. Figure 2.1 show the coordinate system used in the thesis project and the definition of the variables used in oncoming calculations.

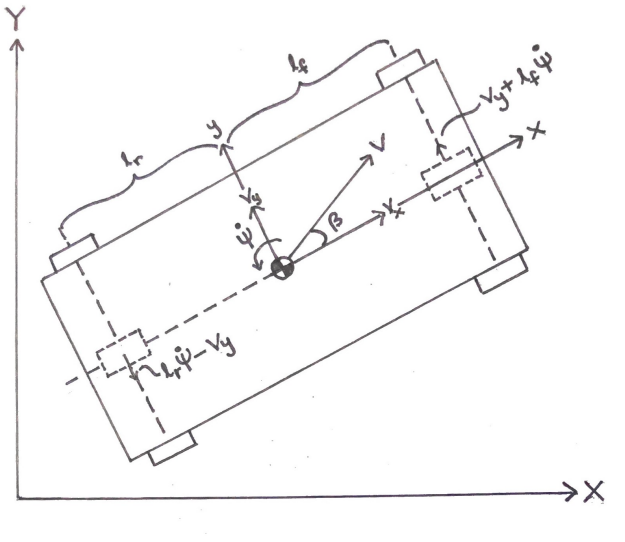

Figure 2.1: *Visualization of the vehicle and coordinate system.*

The side slip angles α_f and α_r for each tire, respectively, can be calculated according to

$$\begin{aligned} \alpha_f &= \delta - \theta_{Vf} \\ \alpha_r &= -\theta_{Vr} \end{aligned} \tag{2.2}$$

where θ_{Vf} and θ_{Vr} are the angles between the longitudinal axis of the vehicle and velocity vector at the front and rear wheel, respectively, and δ is the steering angle of the front wheels. These angles are computed by

$$\begin{aligned} \tan(\theta_{Vf}) &= \frac{v_y + l_f \dot{\psi}}{v_x} \\ \tan(\theta_{Vr}) &= \frac{v_y - l_r \dot{\psi}}{v_x} \end{aligned} \tag{2.3}$$

where v_x is the longitudinal velocity, v_y is the lateral velocity, $\dot{\psi}$ is the yaw rate of the vehicle and l_f and l_r are the lengths between CG and the front and rear axis, respectively [14]. These equations are defined in a different coordinate system compared to the one displayed in Figure 2.1. The difference between the two coordinate systems is shown in Figure 2.2, where the red symbol the original coordinate system for which Equation (2.3) is defined based upon.

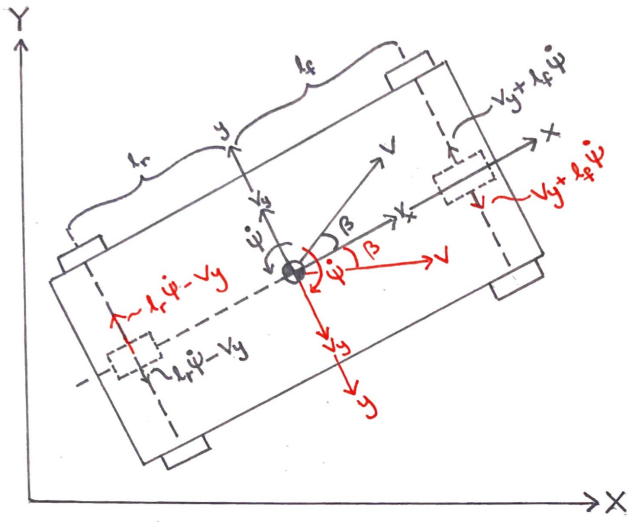

Figure 2.2: *Visualization of vehicle and coordinate system. Coordinate system used for Equation (2.3) is shown in red.*

This means that the corresponding equations for the actual coordinate system are

$$\begin{aligned} \tan(\theta_{Vf}) &= -\frac{v_y + l_f \dot{\psi}}{v_x} \\ \tan(\theta_{Vr}) &= \frac{l_r \dot{\psi} - v_y}{v_x} \end{aligned} \tag{2.4}$$

.

2.2.2 Single-track representation of a 4-wheeled vehicle

The single-track model represents the vehicle on a single axis, with the two front wheels and two rear wheels lumped together. The single-track model is derived from the assumption that both the front and the rear wheel can be steered using the steering angles δ_f and δ_r. In the case of front-wheel steering exclusively, the rear-wheel steering angle δ_r can be set to zero [13]. Since only the front wheel is used for steering, δ will be used instead of δ_f from now on, but does still refer to the front wheel steering angle.

Kinematic single-track model

The kinematic model of a vehicle provides a mathematical description of its motion without considering the forces acting on the vehicle and creating these motions. The equations of motion are therefore only dependent on the geometrical relations of the system. Figure 2.3 describes the kinematics of the lateral vehicle motion.

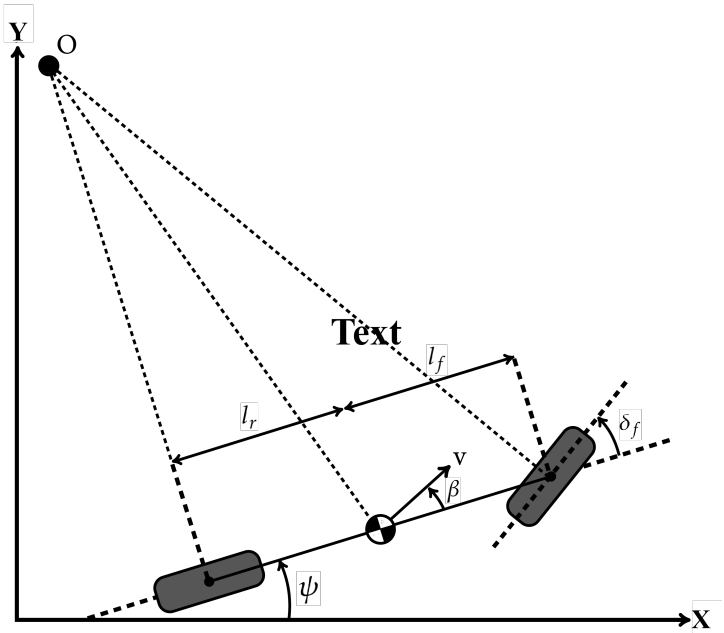

Figure 2.3: *Kinematic single-track model.*

The kinematic single-track model can be considered one of the simplest vehicle models that is frequently used for motion planning. It is used to predict the lateral motion of the vehicle and uses the inertial (X, Y) and the orientation of the vehicle ψ as defined in Figure 2.3 to describe the motion equations of the vehicle [13]. The equations of motion are described by

$$\begin{aligned} \dot{X} &= V\cos(\psi+\beta) \\ \dot{Y} &= V\sin(\psi+\beta) \\ \dot{\psi} &= \frac{V\cos(\beta)}{l_f+l_r}(\tan(\delta_f)-\tan(\delta_r)) \end{aligned} \tag{2.5}$$

where β is the vehicle side slip angle, $\dot{X}$ the longitudinal velocity in the inertial coordinate system and $\dot{Y}$ the lateral velocity in the inertial coordinate system.

The assumptions made for this model are:

- Slip angles at both wheels are zero.
- The steering angles of the right and left wheel are the same.

The first assumption is reasonable to make when the vehicle is moving at low speeds, since low velocity generates a low lateral force on the tires [13]. The second assumption will be discussed further later on.

Dynamic single-track model

When the speed of the vehicle increases, the first assumption made using the kinematic vehicle model can no longer be made. A dynamic single-track model is instead used in this case to model the lateral motion of the vehicle [13]. The dynamic single-track model is shown in Figure 2.4.

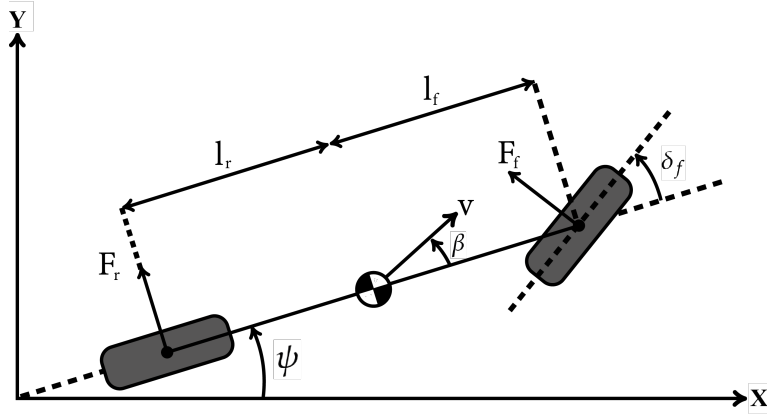

Figure 2.4: *Dynamic single-track model.*

This model is a basic model used for predicting the lateral dynamics of a vehicle. It is useful in situations where the velocity in the longitudinal direction is constant and when slip angles are close to zero [6]. When the slip angle is small, the lateral force applied to a wheel is proportional to the slip angle of the wheel [13].

The two degrees of freedom of the dynamic vehicle model are represented by the lateral position y and the yaw angle ψ [13]. The equations describing the dynamics of a vehicle are

$$\begin{aligned}
\ddot{x} &= \dot{\psi}\dot{y} + a_x \\
\ddot{y} &= -\dot{\psi}\dot{x} + \frac{2}{m}(F_{yf}\cos\delta_f + F_{yr}) \\
\ddot{\psi} &= \frac{2}{I_z}(l_f F_{yf} - l_r F_{yr}) \\
\dot{X} &= \dot{x}\cos\psi - \dot{y}\sin\psi \\
\dot{Y} &= \dot{x}\sin\psi + \dot{y}\cos\psi
\end{aligned} \tag{2.6}$$

where the tire forces F_{yf} and F_{yr} are for a single front and rear tire, respectively, since the equations have taken the wheel lumping together into account by multiplying the forces by two [15]. These forces are computed by using a tire model, which will be presented in Section 2.3.

The assumptions made for the dynamic single-track model are:

- Both the slip angles and steer angles are relatively small [16].
- The steering angles of the right and left wheels are the same.

2.2.3 4-wheeled vehicle with Ackermann steering

One assumption made for the single-track model, because of representing the two front and rear wheels as a single front and rear wheel, is that the steering angles of the right and left wheels are approximately the same. This is not always the case, since the radius of the path that each wheel travels along will differ. The inner wheel will follow a path with a smaller radius than the outer wheel [13].

The steering geometry of a 4-wheeled vehicle with the wheelbase L and the track width B along with the steering angles δ_o and δ_i for the outer and inner wheel, respectively, is shown in Figure 2.5. The solutions to Equation (2.7) is referred to as Ackermann steering geometry [14].

$$\cot\delta_o - \cot\delta_i = \frac{B}{L} \tag{2.7}$$

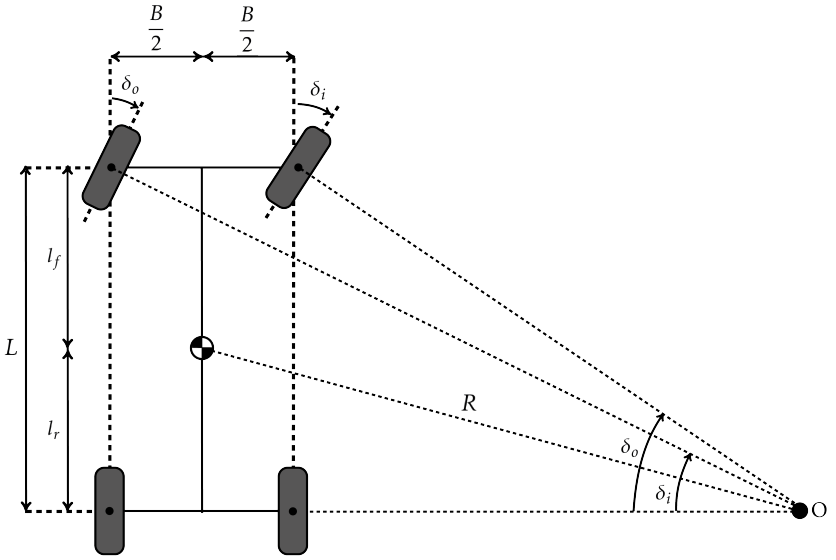

Figure 2.5: *Steering geometry of a 4-wheeled vehicle.*

2.3 Tire models

This section presents some well-known tire models, such as the Magic Formula tire model, HSRI tire model and a linear tire model. These models describe the interaction with the road by modeling the forces and moments created from the tire-road interaction on the contact path between the tire and the road. These forces and moments affect the dynamics of the vehicle [13]. Each tire interacts with the road through the contact path which, because of deformation caused by the vertical load on the tire, is defined as an area that touches the ground at each time instant. The lateral force on the tire is dependent on the amount of lateral deflection present on the threads in the contact patch.

Friction forces act in the opposite direction of the velocity. In presence of a slip angle, and therefore a lateral velocity, the contact patch deforms. The lateral force on the tire depends on the magnitude of lateral deflection of the threads in the contact patch. Hence, for small slip angles, the lateral force is proportional to slip angle[13].

2.3.1 Linear tire model

For small slip angles, the lateral tire forces are proportional to the slip angle of the vehicle. This assumption will not hold for large slip angles; the model will in that case take, e.g., slip angle, normal tire road, tire-road friction coefficient and the longitudinal force into account [13]. The equations describing the linear tire model for small slip angles are described in Equation (2.8).

$$\begin{aligned} F_{yf} &= C_{\alpha,f}\alpha_f \\ F_{yr} &= C_{\alpha,r}\alpha_r \end{aligned} \tag{2.8}$$

The assumptions made for the linear tire model are:

- Slip angles are small.

2.3.2 HSRI tire model

The HSRI tire model is a semi-empirical tire model obtained through experimental testing of tires [17]. This tire model is used in the current version of the Physics Engine of which CARLA is based on.

2.3.3 Pacejka's Magic Formula tire model

The Magic formula is the basis for a widely used semi-empirical tire model used to calculate tire force and moment characteristics of a vehicle. The general form of the tire model is given by.

$$y = D\sin[C\arctan(Bx - E(Bx - \arctan Bx))] \tag{2.9}$$

where the parameters are explained in Table 2.1. The empirical formula is used to produce characteristics that closely resemble measured curves for the lateral force as a function of the slip angle [16].

Table 2.1: *Parameters for Magic Formula Tire Model*

Parameter	Meaning
B	stiffness factor
C	shape factor
D	peak value
E	curvature factor
S_H	horizontal shift
S_V	vertical shift
X	input variable
Y	output variable

2.4 Path planning algorithms

This section provides a description of the path planning algorithms and other relevant theory concerning this subject. A path planning problem is defined as finding a collision-free motion between an initial and final state within a certain environment [18]. An explanation of two relevant algorithms, the A* and the Hybrid A* algorithm, will be provided.

2.4.1 A* and Hybrid A* algorithm

The basic principle of the A* and Hybrid A* algorithms is to represent the environment in a discrete way using an occupancy grid map. An occupancy grid represents a multidimensional space as cells, where each grid space has a probability associated with it [19]. The A* algorithm uses this grid and applies a cost function to estimate the cost to reach each node surrounding the vehicle. The goal of the algorithm is to find an optimal path from the start node s to a goal node t. The path with the minimal cost is constructed by expanding nodes from the start node s and the cost of getting to the current node n and a pointer to the predecessor of n along the lowest cost that far is stored for each node until the goal node is reached. The completed path is then constructed by chaining back from s to t through the pointers [20].

A search algorithm must make decisions about which nodes to expand in order to reach the desired goal node. Expanding nodes which impossibly can be the optimal path is a waste of effort. If the algorithm instead ignores nodes that can lead to an optimal path, it can fail to find such a path and therefore not be admissible. A way to determine which nodes to be expanded is an evaluation function $f(n)$ [20]. The total cost for each node is given by $f(n) = g(n) + h(n)$, where $g(n)$ is the cost of moving to the target node from the current successor node and $h(n)$ is the cost of moving to the next successor node. This method generally only works for holonomic vehicles [21]. Given an 8 by 8 grid surrounding the vehicle as shown in Figure 2.6, the algorithm can steer the vehicle in any direction, independent of its heading. This behaviour is not possible in the presence of nonholonomic constraints [1].

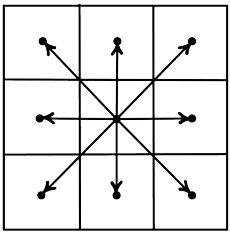

Figure 2.6: *A* algorithm.*

The Hybrid A* algorithm is improved compared to the A* algorithm in order to function for nonholonomic vehicles by predicting the motion of the vehicle and taking that into account when planning the optimal path. This is done by taking speed, gear, steering angle, etc. into account and thereby creating a path to the correct successor node which the nonholonomic vehicle can follow. The cost function for computing the closest path to the target is the same as for the A* algorithm. However, there are additional costs dependent on the motion and moving conditions of the vehicle as well [21]. The input to the algorithm is a

grid, an initial state and a goal state. A state contains the location and orientation of the vehicle. The desired output from the algorithm is a sequence of states forming a trajectory [8].

The path is divided into small segments called motion primitives and they are defined by arcs as shown in Figure 2.7.

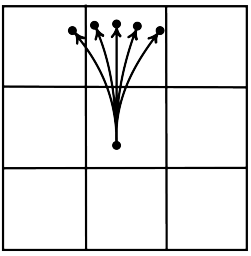

Figure 2.7: *Hybrid A* algorithm.*

The motion primitives have to satisfy the motion equation of the system and do therefore have to fulfill conditions regarding chord length, curvature and heading change. Using the single-track model, the steering angle (α) can be expressed as a function of the chord length (l) and heading change (θ). The formula for computing the steering angle is shown in Equation (2.10) and the possible motion primitives are given by every heading change that generates a steering angle less than α_{max}, which is a tunable parameter [1].

$$\alpha(l, \theta) = \text{atan}\left(\frac{2L}{l} \sin \frac{\theta}{2}\right) \tag{2.10}$$

where L is the wheel base.

2.5 Steering and velocity control

The controller used in the project is a PID controller. In the Autodrive system, the controller is used both to calculate the steering angle and the velocity to be sent to ROS and CARLA. The input to the controller is a reference velocity, which is determined by either choosing a constant value or calculated based on the distance to the goal and the current angular error, and the desired steering angle of the wheels. The output values from the PID controller are translated into steering angles for the wheels and desired torque and these commands are sent to CARLA.

A PID controller generates a control signal $u(t)$ based on the error between the desired and real output from the system, $e(t) = r(t) - y(t)$. The control signal is computed by

$$u(t) = K_P e(t) + K_I \int_0^t e(\tau) d\tau + K_D \frac{d}{dt} e(t) \tag{2.11}$$

where the parameters K_P, K_I and K_D are tunable. A large value on K_P results in a faster following of the reference signal but usually also a decrease in stability margin. An introduction of the integrating term K_I might eliminate stationary error in the output but can also result in a decrease in the stability margin. The derivative term K_D is used to follow changes in the output more quickly, since the derivative of the error is taken into consideration. The derivative term can therefore help in reducing overshoots [22].

3
Method

This chapter describes the method used in the Master Thesis in order to provide an explanation of how the problem at hand was solved. The method consisted of the following elements, where the first item was presented in Section 2 and the remaining items are described in further detail in this chapter:

- Literature study to examine different vehicle models, tire models and the path-planning algorithm. This is presented in Chapter 2.
- Evaluate what changes are possible regarding vehicle models, tire models and vehicle parameters in the simulation environment and physics engine.
- Evaluate if the implementation of the Hybrid A* algorithm is deterministic and find possible sources of error.
- Evaluate which parameters are significant and determine which driving missions to simulate.
- Determine how to measure the performance of the path-planning algorithm and the path following.
- Simulations of said driving missions for a set of different parameters and velocities.
- Compare results and evaluate performance.

3.1 Possibilities of altering vehicle and tire models

The first step of the thesis project was to investigate what changes to the already existing system were possible. The vehicle and tire models are implemented in

the physics engine Unreal Engine which handles all calculations related to the physics in CARLA. There are classes and functions that govern the dynamics of a vehicle and the tires, but altering these would alone well exceed the time limit of this thesis project. Some of the parameters relating to the vehicle modeling were, however, easily accessed in the physics engine and it was therefore decided that the thesis project would shift focus to investigating the behaviour of the vehicle when altering these parameters instead. The vehicle and tire are still very important to keep in mind, and these models were used to investigate the limitations of the implementation of the Hybrid A* algorithm and the equations describing the vehicle dynamics in the physics engine.

3.2 Determinism of the Hybrid A* algorithm

Firstly, it is important to state that this thesis only aims to investigate the implementation of the Hybrid A* in the Autodrive system. No conclusions can be made about the algorithm in a general sense. From this point forward, all mentions of the Hybrid A* algorithm refer to the implementation of the Hybrid A* in the Autodrive system, not the general algorithm.

From initial investigations of the system, trends pointing towards some non-deterministic behaviour were observed and an investigation of the determinism of the Hybrid A* algorithm and the path planner was initiated. The determinism of the Hybrid A* algorithm and the path following are important characteristics, since if the algorithms are concluded to not be deterministic, it is not possible to trust the outcome of a single execution to be representative of the solution in general. In case of a non-deterministic outcome, multiple simulations need to be executed in order to achieve a route that represent reality as close as possible in each case. The characteristics of the path planning and path following were evaluated separately in order to conclude what in the system could, in case of a lack of determinism, be the source of the uncertainty.

Mathematical models can be categorised as either deterministic or stochastic [23]. In order to be considered a deterministic model, the current state must be uniquely determined by the model parameters and the previous state. A deterministic model must therefore produce the same outcome given a set of parameters and initial conditions. The limitations of the deterministic models are that they do not take uncertainty into account. A deterministic model need to be aware of all parameters regarding the governing equations, but this is often not practically reasonable. A system output is often measured discretely and even though the physics are simple there can be issues in trusting the solutions to a deterministic model. Input parameters, initial conditions, model geometry and more are often not completely known and can therefore cause variations in the solution. Stochastic methods can on the other hand be used as a tool to combine the physics, statistics and other uncertainties in the model to describe the system dynamics at hand [23].

In order to determine whether the Hybrid A* algorithm and path following were

deterministic, the same route was driven multiple times in the CARLA simulations using the same parameters and initial conditions. The test route was chosen to be from $(0, 0)$ to $(150, -50)$ in an open world without obstacles and the vehicle and physics parameters were constant throughout all executions. The initial orientation was 0 degrees, which is equivalent to the vehicle pointing directly to the east. An illustration of the test case is shown in Figure 3.2 in Section 3.3.2.

The simulation using the above mentioned route was completed 30 times using the same initial conditions and parameters. The data were collected from the appropriate ROS-topics and saved using a bag-file, which is a file used to store data from a ROS-topic. In order to evaluate the underlying causes of an eventual non-deterministic outcome, the sampling frequencies of the controller and the ROS-bridge were measured.

If the results are collectively the same throughout all sample runs, using the same initial conditions and parameters, it can be concluded that the Hybrid A* algorithm is deterministic and there would only be need for one run in order to collect all necessary data for each test. It is important to establish what is viewed to be a resemblance good enough to be classed as equal and under what conditions the data have been collected. A small difference in position in a non-extreme driving case might affect the result in a more dramatic way when a more extreme driving mission is introduced. The tests were therefore conducted two times using a low and high reference velocity, respectively.

Should the results instead point towards a non-deterministic behaviour, then there needs to be additional assessments made regarding the extracted data. In the case of non-deterministic behaviour where the position varies throughout the executions, it is not possible to draw a direct conclusion from the results since the variation can either depend on the non-determinism or the actual parameter variation. The results need to be presented in a way so that variation from non-deterministic behaviour and parameter alteration can be separated.

If the system is concluded not to be deterministic, the results from the different runs need to be processed to get comparable data. In order to do this, the following conditions need to be fulfilled:

- A known time point in the data set that can be used for synchronization has to exist.
- Each run needs to be identical in the sense that an operation requires the same amount of samples.

If a fixed time point can not be established, it is impossible to synchronize the data. This fixed point would preferably be when the planner is done or when the vehicle start moving. This data point needs to be distinct and identical across all runs. The second item is the most crucial, since if there is a mismatch between the number of samples it takes for example between the vehicle starts moving and reaching the goal, the data in between can not possibly be compared in a numerical manner. If these conditions can not be met, the results will be presented

using scatter plots and if the determinism test should point towards a deterministic system, scatter plots will not be necessary.

In the case that the conditions are met, time synchronization must first be performed. The data sets for all runs are synchronized using the fixed distinct data point, so that the same index of each data set represents the same time instant across all executions. The mean of all data points for one time instant is calculated in order to receive the average value. The way of calculating the mean value properly is dependent on the type of distribution of the values across the runs.

3.3 Determination of simulation cases and driving missions

The driving missions were determined to evaluate the behaviour of the vehicle in both non-extreme and more extreme driving cases in order to investigate how well the models and assumptions made are valid in these cases. As previously described, the Hybrid A* algorithm determines the valid motion primitives using a kinematic single-track model. The assumptions made for this model are that slip angles at both wheels are zero and that the steering angle of the right and left wheels are identical. If these conditions are fulfilled, the Hybrid A* should be able to produce a path that corresponds to a realistic and drivable path for the vehicle. Since the kinematic single-track model is based on the geometry of the vehicle and does not take the tire-road interaction into account, the robustness of the path planning algorithm was evaluated when faced with uncertainties in the vehicle environment.

3.3.1 Determination of significant parameters

The basis for determining the significant parameters in the system was the assumptions made for the vehicle models, tire models and the theory describing the movement of the vehicle. As described in Section 2.2, the assumptions made for the kinematic single-track model are reasonable to make at low velocities, since the slip angle can be assumed to be zero in this case. It was therefore determined that a parameter to consider is the velocity. The reference velocity is specified in the vehicle control. By default, the speed is controlled through a PID-controller. In order to monitor the effects of a low or high velocity, the velocity was set to a constant by setting a constant reference velocity as the input to the PID-controller. An increasing vehicle velocity will theoretically result in an increasing slip angle, since a larger speed will result in both a higher longitudinal and lateral velocity.

The kinematic single-track model does not take the tire-road interaction into account when describing the movement of the vehicle. It was therefore concluded that parameters that directly relate to the environment surrounding the vehicle would be an interesting parameter to investigate in order to evaluate the robustness of the path planning algorithm. The most obvious parameter relating to the

tire-road interaction is the friction between the road and the tire.

When the tires of the vehicle are at the limit of adhesion against the ground, the side slip angle increases and the sensitivity to changes in yaw decreases. When the slip angle increases, a change in the steering angle does not affect the yaw rate of the vehicle greatly. Figure 3.1 shows how a vehicle will behave in a turn for different values of the friction [13].

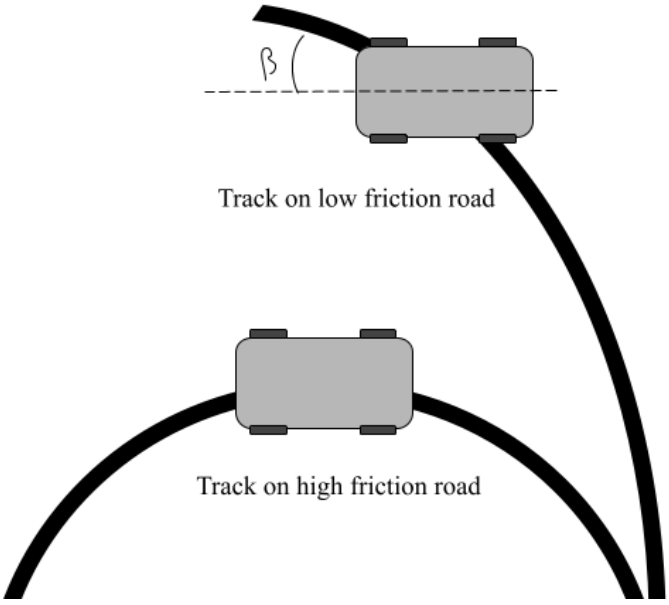

Figure 3.1: *Maneuverability and slip angles of different road surfaces.*

The maneuverability has been found to be lost at slip angles around 10 degrees for dry roads and 4 degrees for snowy roads [13]. Using this knowledge, it will be evaluated how the slip angles vary when altering the friction parameter.

The vehicle mass is also a relevant parameter since it affects the acceleration of the vehicle and is related to the tire-road interaction. The heavier the vehicle, the greater the normal force and therefore more influenced by the friction of the road.

Since one assumption made for the dynamic single-track model is that the steering angles should be relatively small, it was deemed interesting to limit the maximum steering angle that the vehicle is allowed to use. This limitation only applies to the vehicle control, the Hybrid A* could therefore potentially plan a path that requires a steering angle larger than the maximum steering angle allowed in the vehicle control. It will therefore also be evaluated how limitations of the vehicle control affect the vehicle behaviour and how well the planned path can be followed.

3.3.2 Determination of driving missions

The driving missions were determined to evaluate the behaviour of the vehicle in both non-extreme and more extreme driving scenarios in order to investigate how well the models and assumptions made are valid in these cases. As previously described, the Hybrid A* algorithm determines the valid motion primitives using a kinematic model. The assumptions made for this model are that slip angles at both wheels are zero and that the steering angle of the right and left wheels are identical. If these conditions are fulfilled, the Hybrid A* should be able to produce a path that corresponds to a realistic and drivable path for the vehicle. One of the driving missions should therefore be a simple path without any drastic turns and a low maximum speed as well as limiting the steering angle, so that the lateral slip angle will be close to zero. The velocity will be set to a constant of 3 and 5 m/s, since the modeling errors grow larger for velocities larger than that [10]. Using this driving mission, it will be evaluated how different parameters affect the solution of the Hybrid A* algorithm. The first driving mission is illustrated in Figure 3.2.

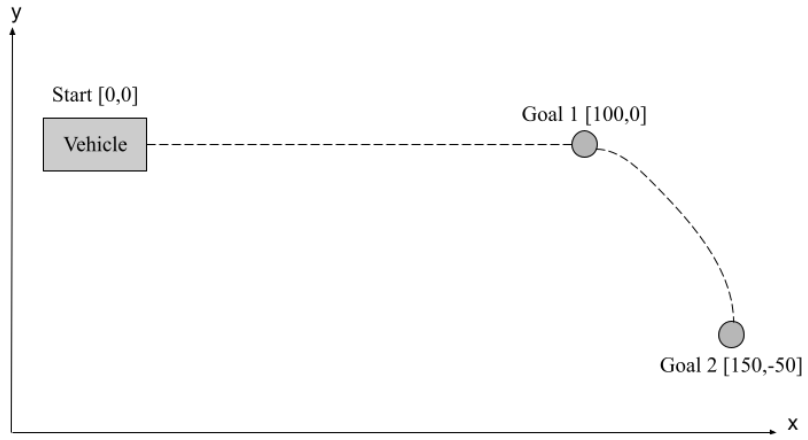

Figure 3.2: *Visualization of DM1.*

The scope of DM1 is:

- Environment: Flat ground without obstacles.
- Start and goal of mission: $(0, 0)$ to $(150, -50)$
- Parameters to limit: Velocity and maximum steering angle.
- Vary: Friction and vehicle mass.

In order to evaluate how the simplification of using the kinematic single-track model affects how well the Hybrid A* algorithm represents a realistic and drivable path, a more extreme driving mission will be designed. In this case, the

assumptions made for the dynamic single-track model will be tested, since a version of a dynamic single-track model is used in the physics engine to describe the motion of the vehicle. As presented earlier, the assumptions made for the dynamic single-track model are that slip angles and steering angles are small and that steering angles for the left and right wheels are equal. The second driving mission will be a more challenging path with a higher maximum speed allowed but limited steering angles. This mission will determine the importance of a more accurate vehicle model. DM2 is illustrated in Figure 3.3.

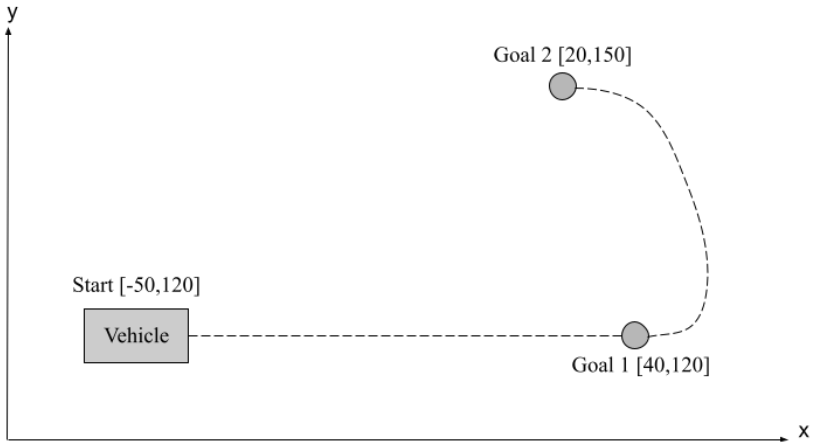

Figure 3.3: *Visualization of DM2.*

The scope of DM2 is:

- Environment: Flat ground without obstacles.
- Start and goal of mission: $(-50, 120)$ to $(40, 120)$
- Parameters to limit: None.
- Vary: Friction, vehicle mass, reference velocity and maximum steering angle.

The third driving mission will investigate how the Hybrid A* algorithm and the vehicle behaviour is affected by realising some limitations from the previous driving missions. The maximum steering angle will be 60 degrees, which mean that the vehicle can steer pretty much as desired. Apart from being longer, DM3 also adds the element of obstacles. This will be simulated in order to determine if the vehicle is suited to handle situations that closely resembles real conditions and how the simplifications of the dynamic vehicle modeling and not knowing the parameters of the environment precisely. In the two previous driving missions, the vehicle did not have to consider re-planning as a result of the occurrence of obstacles. Re-planning is considered by the path planner either when faced with

an obstacle or if the vehicle discovers more of the map than originally having access to. This second aspect of re-planning is discussed further in Section 3.4.3. DM3 is illustrated in Figure 3.4.

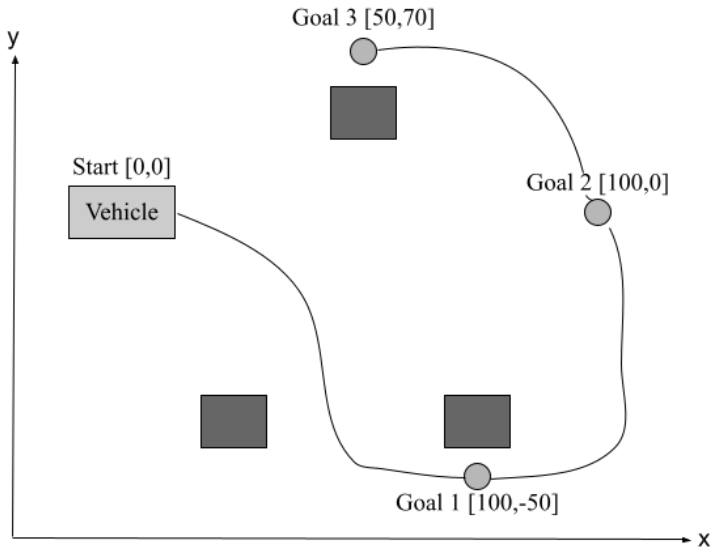

Figure 3.4: *Visualization of DM3.*

The scope of DM3 is:

- Environment: Flat ground with obstacles.
- Start and goal of mission: $(0, 0)$ to $(50, 70)$
- Parameters to contain: Maximum steering angle and reference velocity.
- Vary: Friction and vehicle mass.

3.4 Parameter variations

This section provides a description of how each of the parameters discussed in Section 3.3.1 was altered and which variations were made for each simulation. In order to establish a base-line, the default values in Table 3.1 were used;

Table 3.1: *Default values for each parameter.*

Friction	1μ
Vehicle mass	1500 kg
Ackermann steering	On
Velocity	10 m/s

This thesis project does only take single parameter alterations into consideration. The default values will therefore always be used for all parameters, except the one being altered.

3.4.1 Friction parameter

The friction parameter is represented as a factor of the normal tire friction. The default friction value is 1μ, a decrease to half of the normal is 0.5μ etc. The friction coefficient in the physics engine was first lowered, starting with the standard friction of 1μ and decreasing the value until the vehicle exhibited that it was not able to follow the planned path. This value would determine what would be a suitable lower threshold for the friction parameter. The following parameter values were used as default: 1μ, 0.5μ, 0.1μ, 0.01μ, 1.5μ, 10μ, 50μ. These values were used for DM1. For DM2, it was not possible to use any friction lower than 0.3μ. A test using 0.1μ for DM2 resulted in the vehicle completely drifting off-course and was deemed to not be comparable with the other friction variations. For DM3, this threshold value was chosen to be 0.1μ. The complete selection of parameter choices can be seen in Table 3.4. The friction parameter is set in the physics engine and defines the road characteristics in the simulation environment. It is worth noting that some of the values of the friction parameter are extreme and not relevant to real-life applications, specifically the lowest and highest friction values.

3.4.2 Vehicle mass

The default value of the vehicle mass was decided to be 1500 kg, since this was the pre-determined value in the physics engine. The following values for the vehicle mass parameter were tested for DM1 and DM2: 1500 kg, 1000 kg, 500 kg, 100 kg, 2000 kg, 4000 kg, 10000 kg. For DM3, the 1000 kg and 2000 kg settings were not used and 3000 kg was tested instead of 4000 kg, as seen in Table 3.4. The vehicle mass was set in the physics engine. It is worth noting that some of the values of the vehicle parameter are extreme and not relevant to real-life applications, specifically the lowest and highest vehicle mass values.

3.4.3 Reference velocity

The default value of the reference velocity was decided to be 10 m/s. The velocity was set in the PID controller as a constant value. Usually, the controller decides upon a reference value depending on the driving conditions and distance to the goal, but in order to get consistent settings for the thesis project this value was set to a constant. For DM1 the velocity was chosen to be comparably low, either 3 m/s or 5 m/s, in order to evaluate the variation of the velocity together with altering the friction and mass. In DM2, there were tests done with higher reference velocities. The problem that arose was that the test course only is 400 by 400 m, and the distance of accelerating to anything higher than 10 m/s given the settings made for the vehicle exceeded these 400 m.

One other concern was that the vehicle, as a rule of thumb, is only able to plan approximately 100 m forward, since it is limited by the vision range of the simulated LiDAR. A LiDAR system uses a laser to measure the distance to a target[24]. As presented, DM2 begins at (-50,120), the first waypoint is at (40,120) and ends at (20,150). In this 90 m between the starting point and the first waypoint, it was not possible for the vehicle to accelerate to over 7 m/s. The obvious solution would be to move the starting point further from the first waypoint to provide the vehicle with a longer time to accelerate. This was not possible given the limitations of the LiDAR, since it then will be a need for another waypoint between the new starting point and the first goal at (40,120). For simplicity, assume that the waypoint is placed at the previous starting point, (-50,120). When the vehicle is within the goal range to (-50,120), the Hybrid A* will plan the path towards the first goal point. In order to guarantee that the Hybrid A* algorithm is given the exact same conditions to solve the path planning problem, the vehicle needs to be in the exact same state when the algorithm is solving the problem. If the reference velocity is varied, the vehicle will not have the same speed when reaching (-50,120) and the planned path forward from that point will likely not be identical, or closely similar to one another. In order to compare and draw conclusions from the driven paths, it is crucial that the planned paths are identical or very close to identical. Using trial and error, it was observed that the starting point could be moved to (-80,120) and the Hybrid A* algorithm could still find a straight path to (40,120) using no waypoints in between. The highest reference velocity that will be tested is therefore limited by the maximum velocity the vehicle can reach in the 120 m given the default acceleration limit, which was observed to be 10 m/s. Minor tests of altering the acceleration were performed, but since it was concluded to affect the behaviour in other ways, it was deemed out of the scope of the thesis project.

In conclusion, the velocity variations for driving mission 2 started at (-80,120), with the first waypoint at (40,120) and the goal at (20,150). In both the second and third driving missions, the velocity was altered using the following values: 1 m/s, 3 m/s, 5 m/s and 10 m/s. A test with the reference velocity of 15 m/s was also performed, but with a longer starting distance. The consequences of this will be discussed further in Chapter 5.

3.4.4 Maximum steering angle

The maximum steering angle that was altered in the thesis project is purely related to the path following and was set in the launch file for the chosen vehicle. Alongside this parameter, there is a similar value that defines the boundaries for the Hybrid A* algorithm, but this value was not tampered with. The maximum steering angle was held constant for 10 or 20 degrees for the tests of DM1 but was varied between 5 and 60 degrees for DM2. For DM3, the steering angle was constant at 60 degrees in order to simulate a real-life scenario where a vehicle can steer freely.

3.5 Smoothing of planned path

The general Hybrid A* algorithm is often not optimal and in need of improvements. The paths are empirically found to still be drivable but may contain extra turns which leads to unnecessary steering [7]. This can lead to a planned path that does not represent the driving behaviour of a real-life vehicle. The solution of the algorithm is only based on the fact that each steering angle should be plausible within the limitations of the kinematic single-track model. The possible steering angles are chosen in the interval of $[\delta_{\min}, \delta_{\max}]$ and within that interval there are a number of discretized angles. At each decision point, the algorithm can only choose one of these discrete angles when planning the path, which is the reason the planned path is inherently jerky. The more angles the algorithm has to choose from, the smoother the path.

The version of the path planning algorithm used in the implementation of the system generates the planned path as a series of waypoints, where the distance between each waypoint is a tunable parameter. A larger distance results in fewer waypoints but at the same time less computational power is required for the path planning and path following algorithms. A decreased waypoint distance equals a more precise and smooth path but will in turn increase the computational power needed for the algorithms.

The optimal solution would be a path with enough waypoints to represent the planned path as close as possible to a realistic track, with a good balance between the smoothness associated with fewer waypoints and the accuracy of having more waypoints closer together. The nature of the Hybrid A* algorithm will result in it planning a drivable path given a certain chord length, but the question is how the chord length will affect the planned path and how well the vehicle will be able to follow it. One possible variable to vary is the distance between the waypoints in the planned path. This is done by adjusting the chord length in the Hybrid A* algorithm. The variation of chord length affects how far apart the waypoints were placed, since Hybrid A* use the chord length when determining how far away the next waypoint should be placed. If the chord length is for example 1 m, the distance between two waypoints needs to be at least 1 m. The planner does always have the option of increasing the distance between waypoints, but the chord length parameter determines the minimum value. A large value of the chord length will guarantee a path with largely separated waypoints and therefore also less total number of waypoints. A small value of the chord length will likely result in more tightly placed and more waypoints in total, but it is not guaranteed. The chord length was varied through a factor of the cell size in the occupancy grid and a number of values between 1.5 and 6 meters were tested. The default value was 4.8, which is the value used in all other tests unless anything else is stated. The CPU load was measured for a variety of chord lengths. The test was performed using driving mission 1. This together with the appearance of the path is presented in Chapter 4.

The path following is based on calculating the driving command to a certain reference point, which is treated as the current goal in the path planner. This point

is not necessarily the next waypoint in the list, but is instead determined by a parameter containing an integer. The planned waypoints are stored in a list with the next waypoint in the front. The default value of the look-ahead parameter is 7, which means that the controller will look a number of steps ahead in the list of waypoints and set this value as the current goal for the vehicle control. This value is used for all other tests unless anything else is stated. A smaller number of this parameter will make the path following smoother, since it is not essential to pass through every waypoint that is close by. It does instead calculate the best path to satisfy the route further on, logically resulting in a smoother path. A larger number of this parameter will instead result in the vehicle following the planned route more precisely, but it will at the same time be more sensitive to disturbances. An evaluation of how this parameter affected the smoothness of the path used the same route as for the determinism test, which is described in Section 3.2. The look-ahead parameter was varied between 1 and 10.

One other possibility for smoothing the planned path is a smoothing function. A possible smoothing function for the Hybrid A* algorithm is described in the paper *Practical Search Techniques in Path Planning for Autonomous Driving* [7]. Since this version of the algorithm is based on the use of a Voronoi-field, it is not entirely suitable for the application of this thesis project. Since the scope of the project is not to modify the Hybrid A* algorithm itself, this will not be a part of the project and will only be discussed further in Section 5.5.

3.6 Performance measurement

The performance of the path planner and path following will be evaluated separately, as far as it is possible. Hybrid A* will be evaluated based on its ability to plan a path that is realistic and drivable with respect the current circumstances. The path planner will be evaluated based on how well the vehicle is able to follow the planned path and the limitations of the PID controller. The main focus is to determine how well the Hybrid A* is suited to be used in planning paths without being fully aware of the underlying parameters. Since the controller is responsible for executing the commands provided by Hybrid A*, it is important to understand the limitations of the controller in order to understand the limitations of the path planner.

When looking at the path planner, the following aspects will be considered:

- Position of the vehicle
- Side slip angles
- Rotation of the vehicle

Velocity and side slip angles have been determined to be important factors in how well the vehicle and tire models hold up and are primarily related to evaluating the performance of Hybrid A*. The position of the vehicle is used both in order to evaluate determinism of Hybrid A* and to look at how realistic and drivable a

planned path is in different cases as well as to judge the impact of the controller. Variation of the steering angle is a very important measure in looking at how a mismatch between Hybrid A* and the controller affects the behaviour of the vehicle, since Hybrid A* and the controller have access to different control sets when the maximum steering angle is limited in the controller.

The position is an important factor since it essentially is the result of all underlying effects caused in a specific situation. The position is an important measure of how the vehicle behaves at a larger scale. Some of the aspects might seem very crucial numerically, but will not affect the overall vehicle behaviour largely. The main goal of the autonomous vehicle is in fact to get from one point to another safely. If this is possible will largely be determined by examining the vehicle positions.

3.7 Simulation strategy and data manipulation

This section provides a description of the simulation plan, what data was collected and how this data was processed in order to obtain the wanted quantities. All relevant information regarding the vehicle is received through ROS-topics and is originally extracted from the simulation in CARLA and ROS-bridge. The following data is available through the ROS-topics:

- Planned route: x,y
- Position: x,y,z
- Linear velocity: x,y,z
- Angular velocity: x,y,z
- Acceleration: x,y,z
- Orientation: quaternion
- Control: steer, throttle, brakes, reverse etc.

Table 3.2 shows in which ROS-topics the information is available, where the vehicle status obtains information directly from CARLA and odometry and route information is obtained through the ROS-bridge.

Table 3.2: *Origin of significant data.*

	Odometry	Vehicle Status	Route
Planned route			X
Position	X		
Linear velocity	X		
Angular velocity	X		
Acceleration		X	
Orientation	X	X	
Control inputs		X	

Both the linear and angular velocity is obtained in body-fixed coordinates of the vehicle while the acceleration is described in inertial coordinates. Table 3.3 shows the data that was required for each simulation, the methods to retrieve the data will be described further later in this section.

Table 3.3: *Relevant data from each simulation.*

	Determinism test	Parameter variation	Smoothing tests
CPU/GPU load			X
Position	X	X	X
Linear velocity		X	
Angular velocity		X	

Since some data can be obtained from multiple ROS-topics, it was investigated if data directly from CARLA were identical to the corresponding data from ROS-bridge. Both the linear and angular velocities were calculated using both the pure data from the odometry topic and also using the data obtained from the vehicle status topic. The linear velocity was obtained using

$$v_i = a_i \Delta t + v_{i-1} \tag{3.1}$$

where v_i is the linear velocity at instant i, a_i is the linear acceleration at instant i and Δt is the difference in time between time instant i and i-1. Since the acceleration extracted from the vehicle status topic is obtained in inertial coordinates, the rotational matrix described in Equation (2.6) was used to convert the values to body coordinates. The angular velocity was computed using Equation (3.2). Here, only the computation of $\dot{\psi}$ is described, but the method is identical for the other variables.

$$\dot{\psi} = \frac{\psi_i - \psi_{i-1}}{\Delta t} \tag{3.2}$$

3.7.1 Evaluation of slip angles

The original plan was to utilize the steering angle of the vehicle in order to calculate the slip angles for the front and rear wheels separately. It was later deemed impossible when using the information from the ROS-topics, since the desired steering angle is published, not the real angle of the wheel. Since most of the simulations are done with limitations of the maximum steering angle, the desired and real steering angles will not be the same. Since the calculation of the slip angles for the front wheel requires the steering angle of the front wheel, it is not possible to calculate a realistic value of it. It was therefore decided that only the rear tire side slip angle and the vehicle side slip angle would be used from this point forward. The vehicle side slip angle was calculated using Equation (3.3),

since the vehicle side slip angle is defined as the angle between the longitudinal axis of the vehicle and the orientation of the vehicle velocity vector.

$$\beta = -\arctan\frac{v_y}{v_x} \tag{3.3}$$

3.7.2 Summary of test plan

In summary, the test plan is defined in Table 3.4.

Table 3.4: *Summary of the test plan for the thesis project.*

	DM 1			**DM 2**	**DM 3**
	Test 1	Test 2	Test 3	Test 1	Test 1
Friction [factor of standard friction]	0.05, 0.1, 0.5 1. 1.5, 10, 50	0.05, 0.1, 0.5 1, 1.5, 10, 50	0.05, 0.1, 0.5 1, 1.5, 10, 50	0.3, 0.5, 1 1.5, 10, 50	0.1, 0.5, 1 5, 10
Vehicle mass [kg]	100, 500, 1000 1500, 2000 4000, 10000	100, 500, 1000 1500, 2000 4000, 10000	100, 500, 1000 1500, 2000 4000, 10000	100, 500, 1000 1500, 2000 4000, 10000	100, 500 1500, 3000 10000
Reference velocity [m/s]	5 (constant)	5 (constant)	3 (constant)	1, 3, 5, 10	10 (constant)
Maximum steering angle [deg]	10 (constant)	20 (constant)	10 (constant)	5, 10, 20 40, 60	60 (constant)

For all the parameter variation tests, the deviation between runs will also be estimated in order to observe trends between parameters and deterministic behaviour.

4
Results

This chapter provides the result of the simulations defined in Chapter 3. It will first be evaluated whether the results from the determinism tests point towards a deterministic behaviour, followed by investigating the impact of the smoothing function and finally a presentation of the results from varying the vehicle dynamics parameters and the velocity. The results are primarily presented through plots describing significant variables concerning the vehicle behaviour, such as position, velocity, acceleration and slip angles. The CPU and GPU loads are also important tools in understanding the impact on the computational power and will thus also be presented in relation to the relevant tests. A deeper analysis and connection to the presented theory as well as conclusions from these results will be presented in Chapter 5, this chapter provides the data and other relevant information regarding the simulations.

4.1 Deterministic Hybrid A* and sources of uncertainty

The first task of the thesis project was to determine whether the Hybrid A* algorithm and also the path following were deterministic. As previously described, the system can be considered to be deterministic if the same input conditions and parameters result in the same output. This characteristic is important to consider, since if it is not deterministic, it is not possible to trust one single execution to be representative of the overall behaviour. The test was performed both for the path planning and the path following. The main variable which was used to evaluate the deterministic property of each algorithm was the vehicle position. The tests were done in two different cases, first for a reference velocity of 3 m/s and then

for a reference velocity of 10 m/s in order to evaluate how large the deviation is for non-extreme or more extreme situations.

4.1.1 Reference velocity 3 m/s

The result of the path planning using a constant reference velocity of 3 m/s for 30 different executions is shown in Figure 4.1. The vertical axis represents the y-position and the horizontal axis represents the x-position. If nothing else is stated, the unit can be assumed to be in meters.

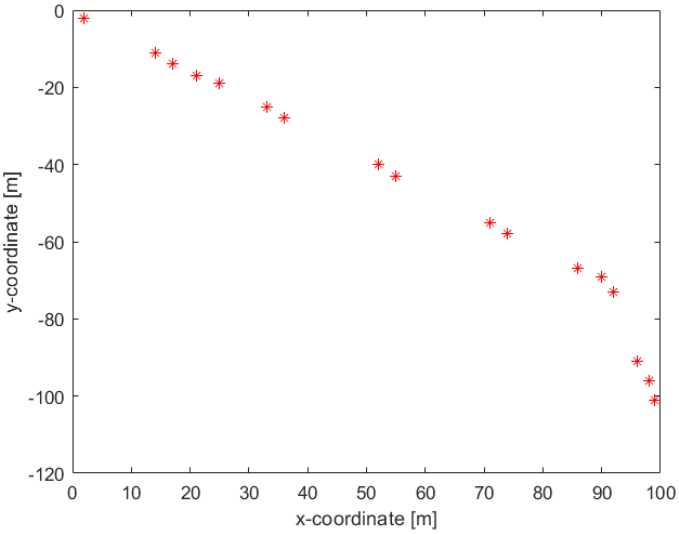

Figure 4.1: *Planned route for reference velocity 3 m/s, 30 different runs. The resulting waypoints for each simulation are placed directly on top of each other.*

Each dot in Figure 4.1 represents a waypoint in the planned route. The default setting provides a planned route with largely separated waypoints at times, which leave a big room for the vehicle control to create a reasonable path between each waypoint. As the figure shows, the planned path is the same throughout all executions, since all the waypoints are located at the exact same positions. Using this test, it can be concluded that the route planning, given the exact same conditions when planning, will result in the same planned route every time. The actual route the vehicle followed for the corresponding case is shown in Figure 4.2.

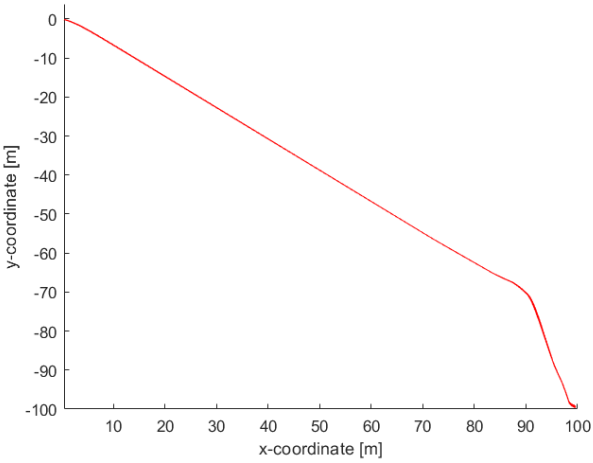

Figure 4.2: *Real route for reference velocity 3 m/s, 30 different runs.*

It can be observed that the followed path over the 30 executions looks roughly identical throughout the majority of the course, but deviates more or less in certain portions of the path. In particular, there is a comparably larger deviation between the runs during the turn at approximately (90,70). Figure 4.3 shows the last portion of the course, where the vehicle experiences a right turn. In this figure, the distribution of positions is visualized using a scatter plot where each data point is represented by an opaque dot. A darker color therefore corresponds to a higher amount of data points in that certain location.

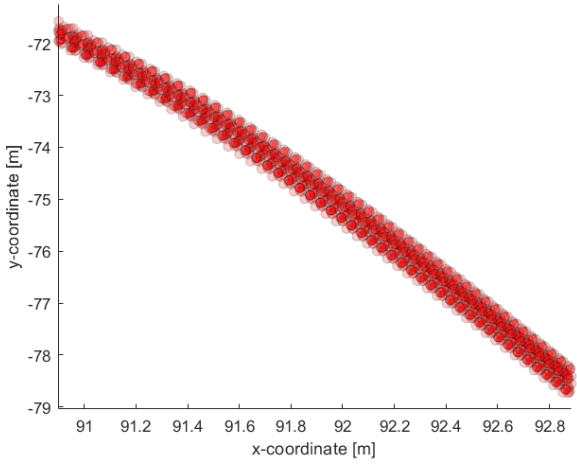

Figure 4.3: *Real route for reference velocity 3 m/s, 30 different runs.*

By looking at Figure 4.3, the deviation in position is roughly a few decimeters at most between the 30 runs that were executed. This means that the vehicle position for this case can be assumed to be within this interval. In order to achieve some type of statistical basis of how the position deviation is distributed, a much larger quantity of tests is of course required. During the portions of the course where the vehicle was going straight, the deviation was negligible.

4.1.2 Reference velocity 10 m/s

The second test case was to determine whether a larger reference velocity resulted in a larger variance between different executions. In total 30 runs were performed with a reference velocity of 10 m/s. Figure 4.4 shows the planned path for this test case.

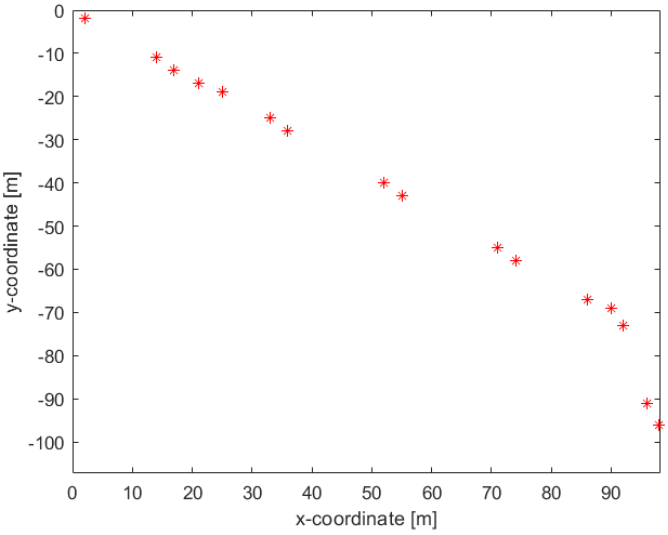

Figure 4.4: *Planned route for reference velocity 10 m/s, 30 different runs. The resulting waypoints for each simulation are placed directly on top of each other.*

The planned path is identical between all 30 runs. The planned path does not seem to differ between the case with reference velocity 3 m/s, the locations of the waypoints are identical. The followed path for reference velocity 10 m/s is shown in Figure 4.5.

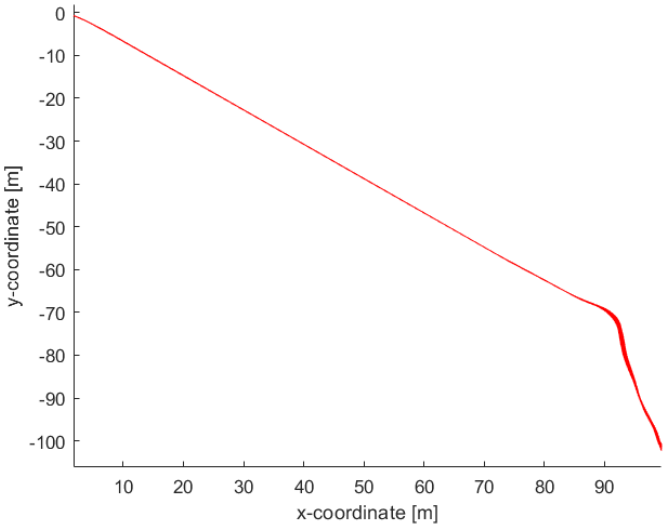

Figure 4.5: *Real route for reference velocity 10 m/s, 30 different runs.*

The positions are identical during the parts of the course where the vehicle is driving straight. During the turns, the positions seem to deviate between the 30 runs. Figure 4.6 shows the right turn at approximately (90,70), using the scatter plot where a darker color represent a higher concentration of data points.

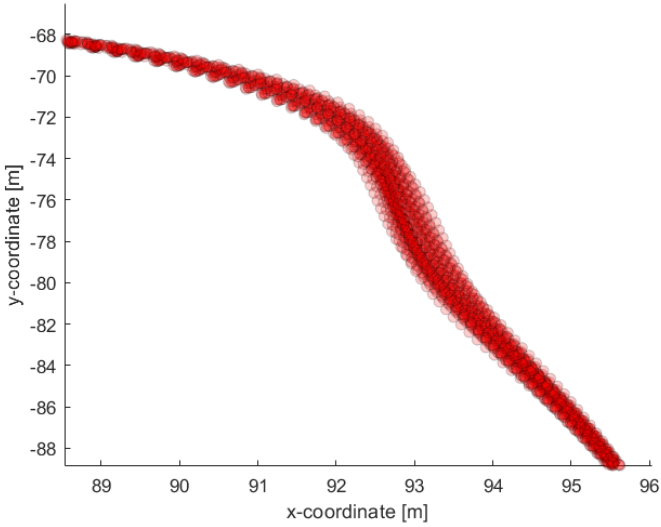

Figure 4.6: *Real route for reference velocity 10 m/s, 30 different runs.*

In this case, the difference between the runs was around a meter. The vehicle position can be assumed to be somewhere within this interval when using the reference velocity 10 m/s.

4.1.3 Conclusions regarding determinism and data manipulation

Since the results point towards a non-deterministic behaviour, multiple runs were needed in order to observe the vehicle behaviour in the tests to come. It was also concluded that no fixed data point or consistency in run length could be established, and the results will therefore be presented using scatter plots. The most significant problem was that the non-determinism resulted in that velocity and other factors varied between the runs, and each execution did therefore have inconsistent lengths.

4.1.4 Sampling frequencies for subsystems

Since the path following was deemed not to be deterministic over different simulations, it was investigated what some probable causes of this observation could be. In order to investigate if discord between the subsystems CARLA, ROS, ROS-Bridge and Autodrive occurs, the sampling rates were measured. Time stamps for the PID controller and ROS-Bridge were collected for each iteration of the respective subsystem, when using the default settings for DM1. The time stamp for each sample was recorded and the difference between two samples was calculated in order to receive an absolute time difference. The sampling periods for the controller is displayed in Figure 4.7.

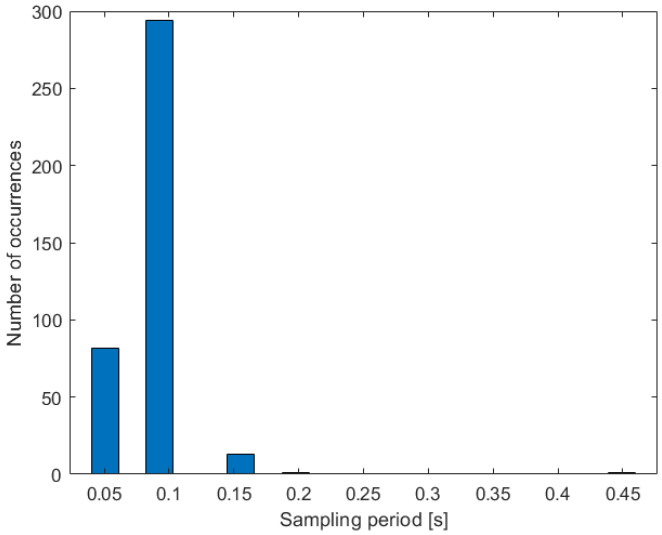

Figure 4.7: *Distribution of sampling periods for the Controller.*

The sampling periods vary mainly between 0.05 s and 0.15 s, with the majority of samples taken with a sampling period of 0.1 s. There are, however, some instances of larger sampling periods of 0.2 s and 0.45 s. The sampling periods for the ROS-Bridge are shown in Figure 4.8.

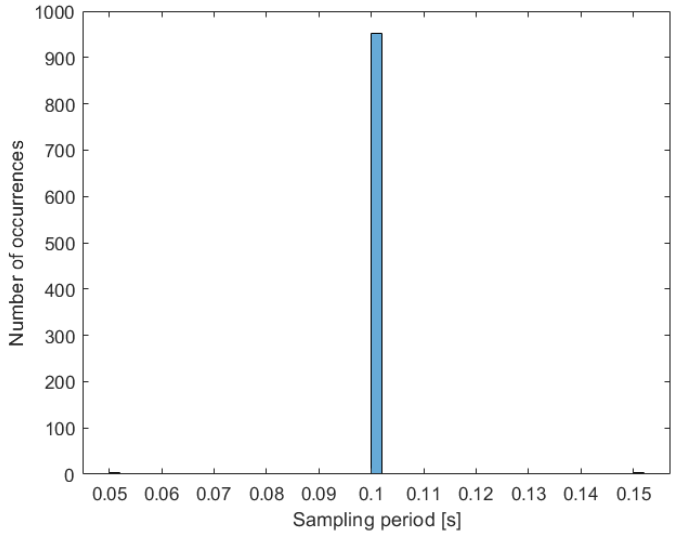

Figure 4.8: *Distribution of sampling periods for the ROS-Bridge.*

An overwhelming majority of the samples are collected with a sampling period of 0.1 s, apart from some isolated samples with a sampling period of 0.05 s or 0.15 s. Through both these tests, it can be assumed that both the controller and the ROS-bridge largely runs on the sampling frequency of 10 Hz. Even though the sampling periods were not consistent, they did always assume a discreet value with the period 0.05 s, for example 0.05 s, 0.1 s, 0.15 s etc.

4.2 Smoothing of planned path

Two methods were used in order to evaluate the possibility to make the solution from the Hybrid A* algorithm smoother and consequently more realistic and comparable to the actual desired behaviour of a vehicle. This section is focused on the implementation of the path planner, and ignores any data concerning the actual followed path.

4.2.1 Variation of chord length

Some initial simulations were performed in order to investigate the magnitude of the deviation between runs when varying the chord length. The results from

varying the chord length were not affected greatly by the non-deterministic behaviour of the system, so in order to obtain a reasonable visualization, only one set of data was plotted for each parameter variation. Figure 4.9 shows the position of the vehicle during this test. The pink line is a chord length of 1.5 m, the green 3.3 m, the black 4.8 m and the blue 6 m. The dots in the respective colour represent the planned route for the vehicle for each case.

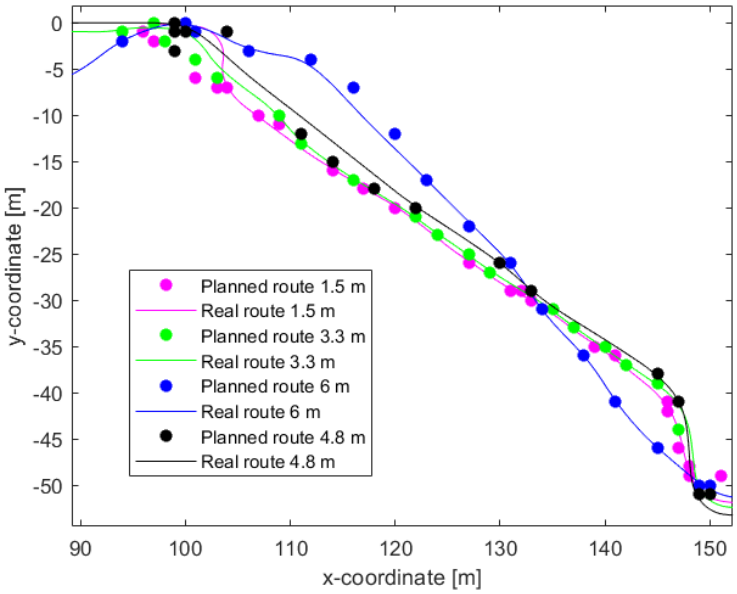

Figure 4.9: *Chord length variation for DM1.*

For the chord lengths of 1.5 m and 3.3 m, the waypoints are generally closer together for most of the route and the vehicle seems to more closely follow the planned path. For the chord length 6 m, the planned path deviates greatly from the other cases. The route for this case is straighter and does not follow the same pattern as for the lower chord lengths. Looking at the black dots, which represent the default chord length of 4.8 m, the path planner exhibits an interesting behaviour at around coordinate (100,0) which will be discussed further in Chapter 5.

The CPU load was monitored during the chord length variations, but no obvious trends about how the chord length affected the CPU-load could be observed. Since the CPU load varied greatly between each run, there could not be placed a numerical value for each chord length variation and no comparisons could be made.

4.2.2 Controller look-ahead

The results from altering the look-ahead parameter are shown in Figure 4.10. As described in Chapter 3, the look-ahead parameter represents how far ahead the vehicle control will look in the list of waypoints when determining the next goal state. A small value of this parameter results in the vehicle control looking far ahead and therefore ignoring some waypoints. A large value will result in the vehicle looking very closely ahead and therefore reaching almost all waypoints. The pink dots represent the value 1, the green 3, the yellow 7 and the red 10. The black markings represent the planned path, which is identical for all cases since this parameter does not affect the path planner in any way.

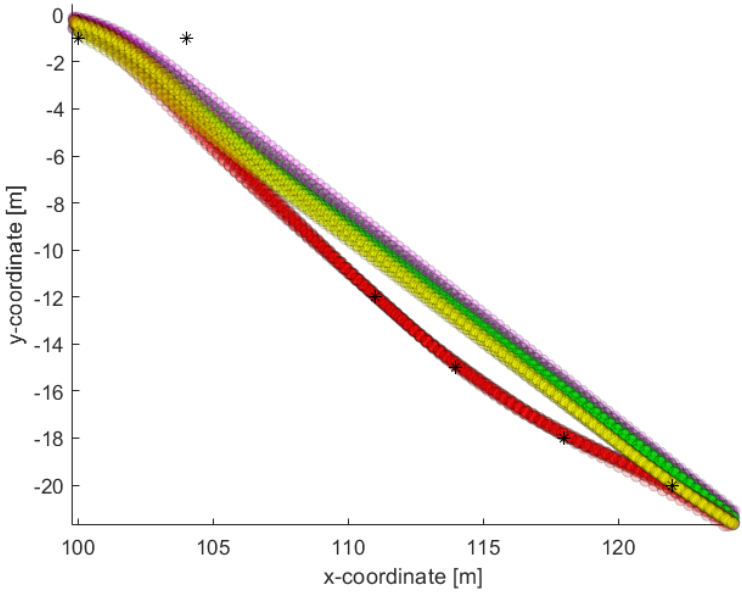

Figure 4.10: *Look-ahead parameter variation for DM1.*

A higher value of the parameter results in a closer following of the planned path. During the turn that is shown in Figure 4.10, the red line is the only configuration where the vehicle takes the waypoints at approximately $[111, -12]$, $[114, -15]$ and $[117, -18]$ into consideration. With the look-ahead parameter 7, which is represented with the yellow line, the vehicle seems to pass through the waypoint at approximately $[122, -20]$, but this waypoint is disregarded for the lower values of the look-ahead parameter.

The same observation regarding the CPU loads for the chord length variation applies to the look-ahead parameter variations. No obvious trend could be observed about how varying the look-ahead number affects the CPU load of the computer.

4.3 Variation of vehicle dynamics parameters

This section provides the results when varying different parameters tied to the vehicle dynamics. As described in Section 3, the following parameters were investigated in three different driving missions: tire friction, vehicle mass, maximum steering angle and reference velocity. The results will be visualized using scatter plots containing data from 10 different runs for each test case, since there the factor of non-deterministic behaviour prevents the vehicle behaviour to be represented by a single execution.

Results regarding the vehicle behaviour not directly visible from the position plots are presented in one table for each parameter. The data presented in these tables are minimum and maximum vehicle side slip angle, side slip angle at the rear tire, yaw rate and the deviation between runs for a certain parameter variation during a specific portion of the course. It is also presented which configuration resulted in the obtained value. This is used to give a rough understanding of trends in vehicle behaviour when varying the parameter. The full test results are available in Appendix A. For both driving missions 1 and 2, the values are calculated from the first major turn of the driving mission. All figures presenting the position of the vehicle in this section will display the results during this same major turn, since the effects from varying the parameter did not translate when the vehicle was driving along a straight line. Neither did it affect the side slip angles, yaw rate or deviation between runs, which all were negligible when driving straight.

Due to the non-deterministic behaviour, the table values are victim to uncertainty and extracted only from a rough estimation of the slip angles, yaw rates and deviation between runs. In some cases, the variables vary greatly between runs and the estimation of the mean value might not represent the real-life value. If the minimum and maximum slip angle is within a few degrees and especially if the value does not seem to follow a pattern when the parameter is varied, then the result will be discarded because of uncertainty.

During the simulation of DM2, it was determined that the vehicle was not able to accelerate quickly enough to reach the default reference velocity of 10 m/s, because of a too short acceleration distance. The maximum velocity reached approximately 7 m/s, but was consistent and was assessed to not affect the results, as long as the reference velocity and acceleration distance were constant throughout the simulations. The tests where the velocity is altered are the exceptions, since it was important to reach the desired velocity. During the velocity simulations, the acceleration distance was instead altered.

DM3 was special in the aspect that there were obstacles present and the vehicle needed to re-plan during the mission, as described in Chapter 3. The results from this driving mission will be presented visually but will not be included in the data tables.

4.3.1 Tire friction

As previously described, the friction parameter was altered for all three driving missions and a selection of the results is presented in Table 4.1. It contains minimum and maximum values for the side slip angles, yaw rate and the magnitude of deviation between runs also. The value and the corresponding parameter for which the value was achieved are presented in the table.

Table 4.1: *Results from altering friction parameter.*

	DM 1 - During Curve			**DM 2**
	Test 1	Test 2	Test 3	Test 1
Minimum $\lvert\beta\rvert$ [deg]	6 (0.05μ)	6 (0.05μ)	6 (0.05μ)	22 (0.3μ)
Maximum $\lvert\beta\rvert$ [deg]	19 (multiple)	19 (1.5μ)	20 (multiple)	26 (multiple)
Minimum $\lvert\alpha_r\rvert$ [deg]	3.5 (0.1μ)	3.5 (0.1μ)	5 (0.05μ)	5.5 (0.3μ)
Maximum $\lvert\alpha_r\rvert$ [deg]	6.5 (0.05μ)	6.5 (0.05μ)	7 (multiple)	7.5 (multiple)
Minimum $\lvert\dot{\psi}\rvert$ [deg/s]	20 (0.05μ)	20 (0.05μ)	20 (0.05μ)	75 (0.3μ)
Maximum $\lvert\dot{\psi}\rvert$ [deg/s]	45 (multiple)	45 (multiple)	27 (50μ)	90 (multiple)
Minimum deviation between runs [m]	0.5-1 (multiple)	0.5-1 (0.5μ)	0.2 (multiple)	≈ 0.5 (10μ)
Maximum deviation between runs [m]	1.5-2 (0.05μ)	1-1.5 (1.5μ)	≈ 1 (50μ)	≈ 1.5 (1μ)

From Table 4.1 it can be seen that the minimum vehicle side slip angle and yaw rates were consistently obtained for the lowest friction parameter, while multiple parameter choices resulted in the same value for the maximum vehicle side slip angle and yaw rate. The minimum and maximum side slip angles for the rear tire and deviation between runs varied depending on the test and driving mission.

Figure 4.11 shows the position of the vehicle from a small section of the course, when performing the first test of DM1. The red dots represent a friction of 0.1μ, the light blue dots 0.05μ and the remaining dots are values between 0.5 and 50μ where the yellow line is the default run.

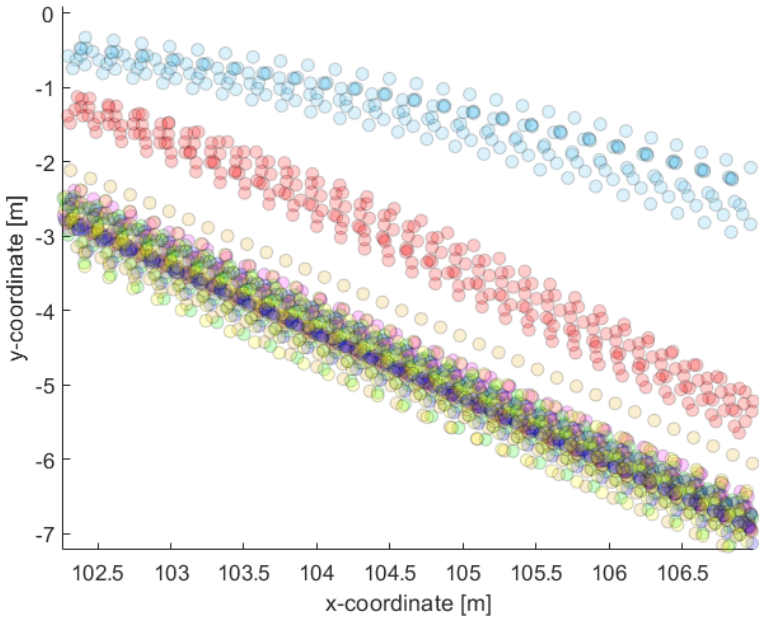

Figure 4.11: *Friction variation for first test of DM1.*

From Figure 4.11 it can be observed that the light blue dots (0.05 μ) and red dots (0.1 μ) deviate from the other configurations. Apart from this, it is not possible to draw any clear conclusions regarding the other parameter values, since they all fall into the interval of variations resulting from non-deterministic behaviour. It therefore seems that a friction below 10% of the normal friction clearly results in the vehicle drifting apart from the original path, while there is no major effect when using the other parameter settings.

The same trend applies for the second and the third test of DM1 as well, where the second test gave near identical results as the first test. The positions of the vehicle for the third test of DM1 are shown in Figure 4.12. The red dots represent a friction of 0.1 μ, the light blue dots 0.05 μ and the remaining dots are values between 0.5 and 50 μ where the yellow line is the default run.

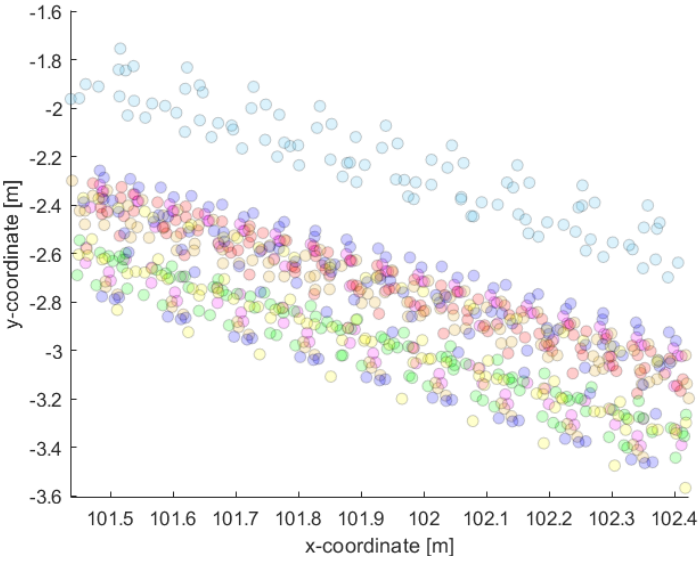

Figure 4.12: *Friction variation for third test of DM1.*

It is still possible to observe that a lowered friction resulted in the vehicle drifting, but by much smaller distances compared to the first and second tests. The light blue dots (0.05μ) are still deviating from the other configurations, but it is harder to separate the red dots (0.1μ) from the other parameter settings. Figure 4.13 shows the results in the main U-turn of DM2.

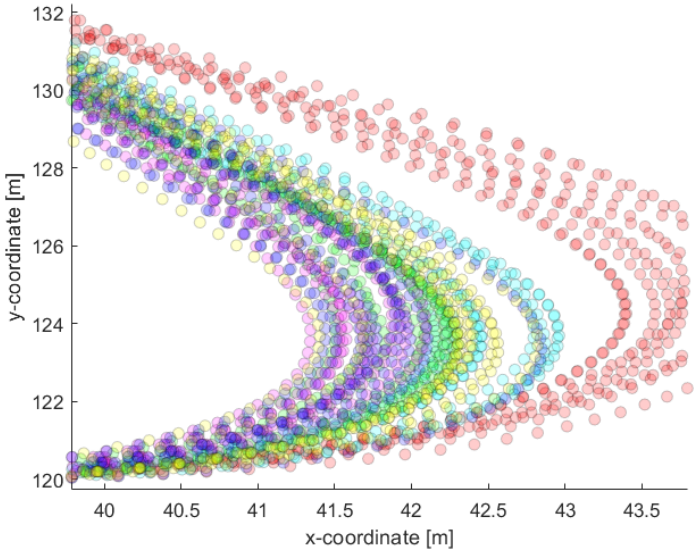

Figure 4.13: *Friction variation for DM2.*

The red dots represent 0.3μ, and the position of the vehicle deviates heavily compared to the other parameter settings. The same behaviour can be seen in the light blue dots, which represent 0.5μ. The yellow dots represent the default configuration, the green dots 1.5μ, the magenta dots 10μ and the dark blue dots 50μ. The general trend, which can be determined by observing where the respective colour is more prominent, in the test is that a lower friction, represented mainly by the red and light blue dots, results in the vehicle following a wider curve during the turn.

Figure 4.14 shows the planned route for DM3 and Figure 4.15 shows the results of the friction variation, where the red dots represent 0.1μ and the light blue dots represent 0.5μ. The yellow dots represent the default configuration, the green dots 1.5μ, the magenta dots 10μ and the dark blue dots 50μ.

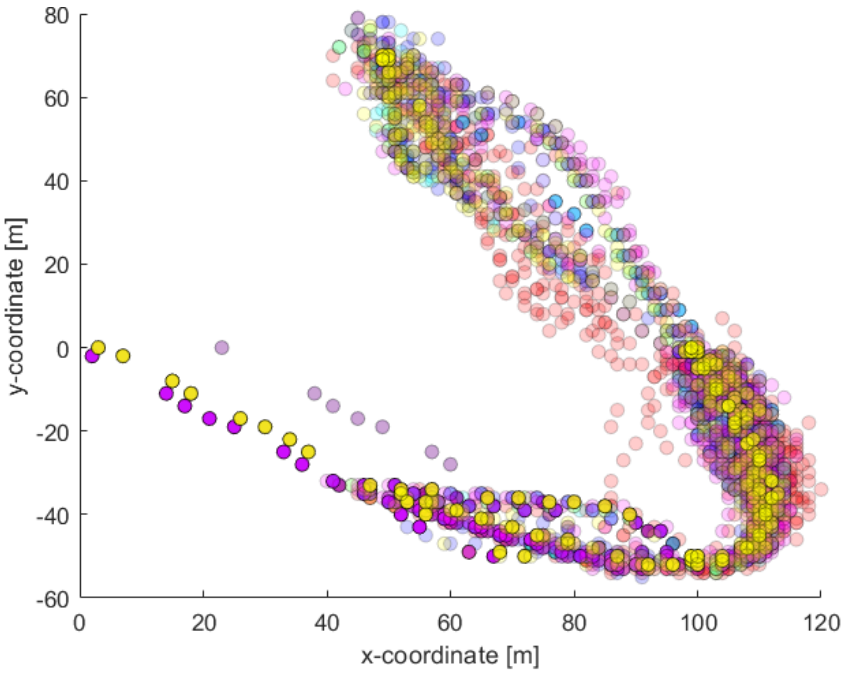

Figure 4.14: *Planned path, friction variations for DM3.*

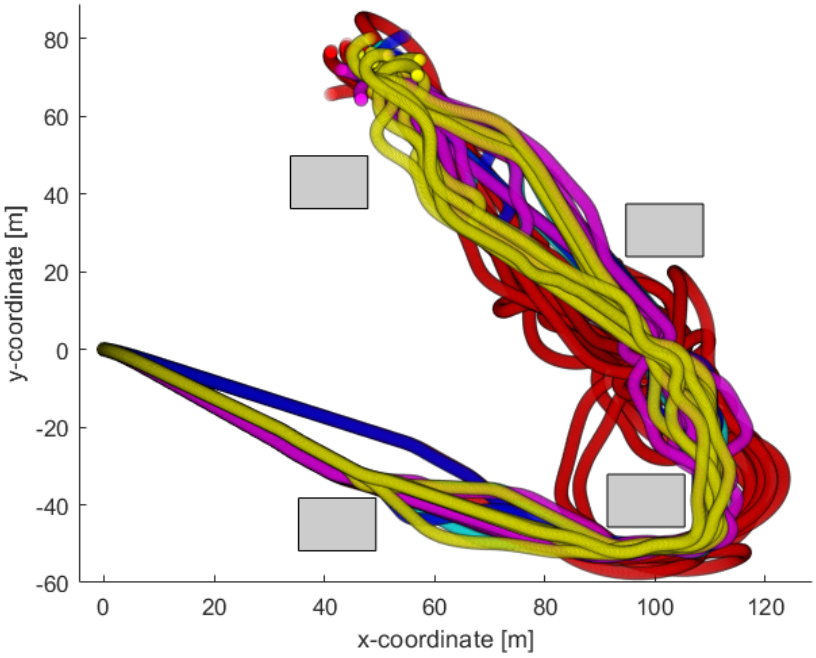

Figure 4.15: *Real path, friction variation for DM3. The grey boxes shows the approximate locations of the obstacles.*

The planned path for DM3 is very different for each execution. All planned paths follow the same pattern because of that the goal waypoints are identical. The deviation of the planned path is a result of the nature of the test, which provides more room for the vehicle to explore its environments freely. The effects of this will be discussed further in Chapter 5. By looking at Figure 4.15, the red dots (0.1μ) are very different from the remaining ones since the vehicle with this configuration drifted away from the path and decided to drive back around the obstacle. Apart from this, no other clear trends can be seen from the figure.

When determining which parameters should be tested for DM2, the friction 0.1μ was also tested but was deemed too low for the vehicle to complete the mission successfully. One significant result is that α_r reached a value of approximately 80 degrees during the first turn of the mission. This is a very large slip angle and it is equivalent to the vehicle drifting almost completely sideways.

4.3.2 Vehicle mass

In the same manner as for the friction parameter variations, the results regarding the velocity profile, the vehicle side slip angle, side slip angle at the rear tire, yaw rate and the deviations because of non-determinism are shown in Table 4.2.

Table 4.2: *Results from altering vehicle mass parameter.*

	DM 1			**DM 2**
	Test 1	Test 2	Test 3	Test 1
Minimum $\lvert\beta\rvert$ [deg]	18 (10000 kg)	18 (4000 kg, 10000 kg)	20 (all)	24 (500 kg)
Maximum $\lvert\beta\rvert$ [deg]	19.5 (100 kg)	19 (100 kg)	20 (all)	26 (multiple)
Minimum $\lvert\alpha_r\rvert$ [deg]	5 (10000 kg)	5.5 (multiple)	7 (all)	5.5 (500 kg)
Maximum $\lvert\alpha_r\rvert$ [deg]	6.5 (100 kg)	6 (100 kg)	7 (all)	8.5 (100 kg)
Minimum $\lvert\dot{\psi}\rvert$ [deg/s]	3.3 (500 kg)	44 (multiple)	26 (multiple)	85 (10000 kg)
Maximum $\lvert\dot{\psi}\rvert$ [deg/s]	47 (100 kg)	47 (100 kg)	28 (multiple)	93 (100 kg)
Minimum deviation between runs [m]	0.5-1 (100 kg)	≈ 1 (100-4000 kg)	≈ 0.5 (100-4000 kg)	≈ 0.5 (500 kg)
Maximum deviation between runs [m]	1-2 (10000 kg)	1-1.5 (10000 kg)	≈ 1 (10000 kg)	1.5-2 (multiple)

The minimum vehicle side slip angle and yaw rate were generally obtained for the mass 10000 kg and the maximum for 100 kg but this result was not consistent for all driving missions. The maximum side slip angle at the rear tire was usually obtained for mass 100 kg, but no certain trend can be seen regarding the maximum values. The deviation between runs was generally higher for a larger vehicle mass and lower for a smaller mass.

For the first and third simulation of DM1 no conclusions could be made from looking at the position of the vehicle, since the changes from changing the parameter were within the interval of deviation due to non-determinism. This applied to all values of the mass parameter. For the second test, the effects of varying the mass parameter were still very small, but some trends can be seen in Figure 4.16.

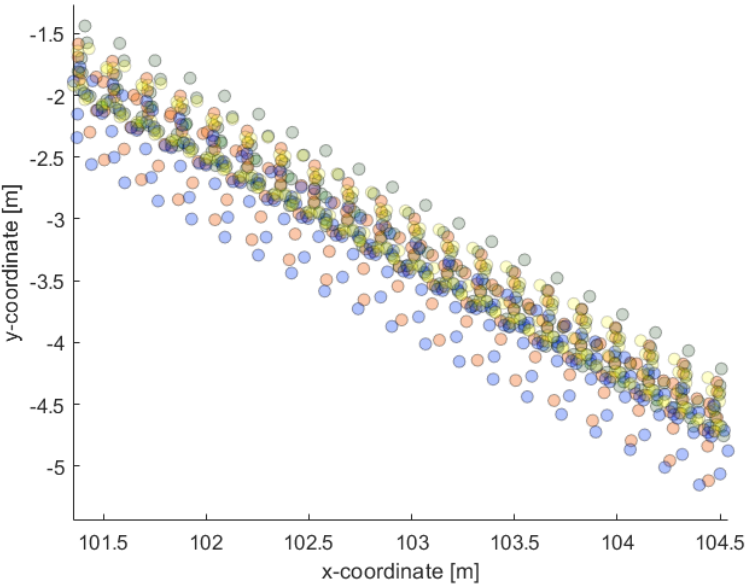

Figure 4.16: *Vehicle mass variation for second test of DM1.*

By looking at Figure 4.16, where the blue dots represent the heaviest vehicle configuration with 10000 kg, the trend seems to point towards the vehicle taking a steeper turn during this case. Figure 4.17 shows the vehicle positions for DM2.

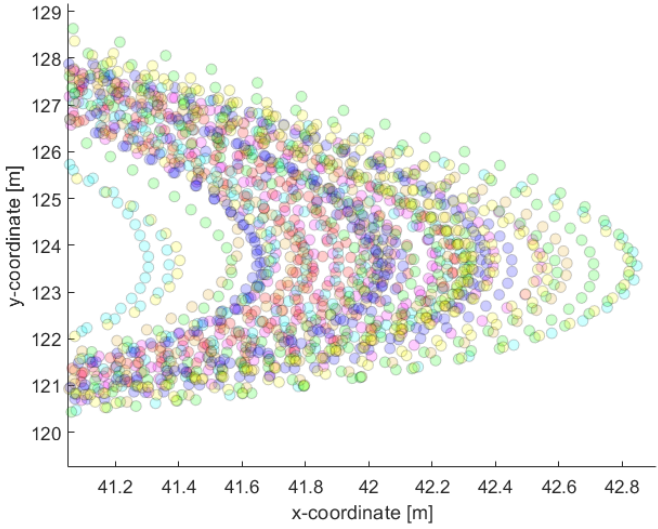

Figure 4.17: *Vehicle mass variation for DM2.*

No obvious trends regarding the behaviour of the configurations can be drawn from this figure, since all alterations fall into the interval of deviation between the runs. Figure 4.18 shows the position of the vehicle when the mass is varied for DM3.

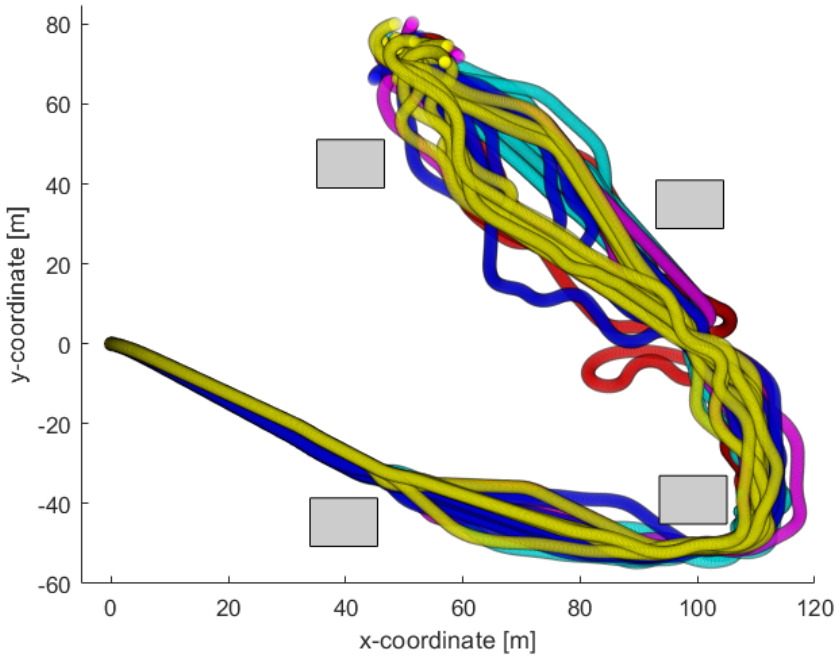

Figure 4.18: *Real path, vehicle mass variation for DM2. The grey boxes shows the approximate locations of the obstacles.*

Nothing can be said about how varying the vehicle mass parameter affect the vehicle position. This is because of the inconsistent path planning, which is a result of the path following not being deterministic and therefore failing to provide the path planner with the same initial conditions for each run.

4.3.3 Reference velocity

Table 4.3 shows the results regarding the slip angles, yaw rate and deviation between runs from varying the reference velocity which is sent to the PID controller.

Table 4.3: *Results from altering reference velocity.*

	DM 2
Minimum $\lvert\beta\rvert$ [deg]	16 (15 m/s)
Maximum $\lvert\beta\rvert$ [deg]	34 (1 m/s)
Minimum $\lvert\alpha_r\rvert$ [deg]	5.5 (10 m/s)
Maximum $\lvert\alpha_r\rvert$ [deg]	14 (1 m/s)
Minimum $\lvert\dot{\psi}\rvert$ [deg/s]	15 (1 m/s)
Maximum $\lvert\dot{\psi}\rvert$ [deg/s]	124 (15 m/s)
Minimum deviation between runs [m]	$\approx$ 1 (multiple)
Maximum deviation between runs [m]	$\approx$ 3 (15 m/s)

From Table 4.3 it can be seen that the side slip angles increase with a decreasing velocity, while the yaw rate and deviation between runs increases with an increasing velocity.

Figure 4.19 shows the position of the vehicle throughout the main U-turn of DM2 while varying the reference velocity. The red dots represent 1 m/s, the light blue dots 3 m/s, the green dots 5 m/s, the yellow dots 10 m/s and the pink dots 15 m/s.

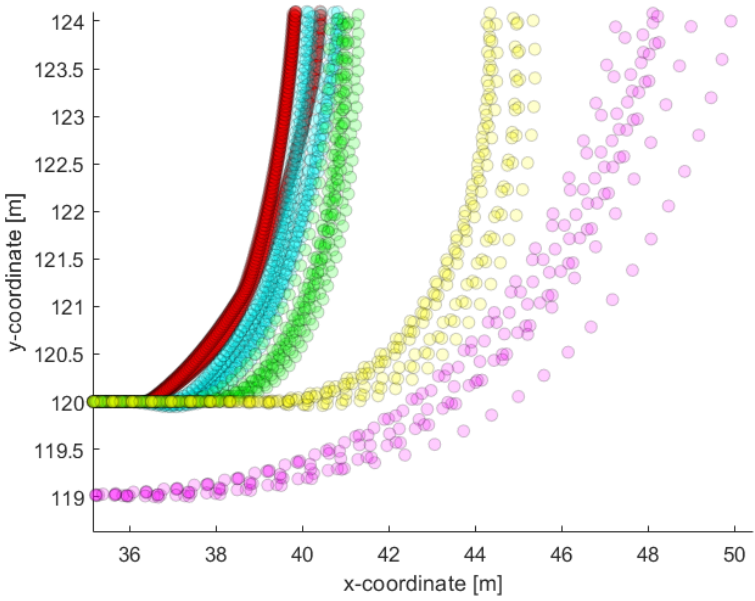

Figure 4.19: *Reference velocity variation for DM2.*

From the most dynamic part of the turn, the difference between 1 m/s and 3 m/s is approximately a meter. At 5 m/s, the difference in position increases slightly

and when driving at 10 m/s the vehicle drifts significantly from the intended path. The position differs by a few meters compared when driving at lower velocities. For the largest velocity of 15 m/s, the vehicle needed more distance to accelerate and the planned path did vary slightly from the planned path of the other configurations. Even though it is not possible to compare these results any further because of this, it can clearly be seen that the vehicle drifts heavily in this case.

4.3.4 Maximum steering angle

Table 4.4 shows the maximum velocity, vehicle side slip angles, side slip angle at the rear tire, yaw rate and the deviation between the runs for the maximum steering angle test.

Table 4.4: *Results from altering the maximum steering angle.*

	DM 2
Minimum $\lvert\beta\rvert$ [deg]	25 (multiple)
Maximum $\lvert\beta\rvert$ [deg]	26 (multiple)
Minimum $\lvert\alpha_r\rvert$ [deg]	6 (60 deg)
Maximum $\lvert\alpha_r\rvert$ [deg]	7 (multiple)
Minimum $\lvert\dot{\psi}\rvert$ [deg/s]	87 (multiple)
Maximum $\lvert\dot{\psi}\rvert$ [deg/s]	90 (multiple)
Minimum deviation between runs [m]	≈ 1 (multiple)
Maximum deviation between runs [m]	≈ 1.5 (multiple)

By looking at Table 4.4, the values do not deviate much between each configuration, which point towards the maximum steering angle not impacting these variables much. It can be seen that the minimum side slip angle at the rear tire is lowest for the maximum steering angle 60 degrees.

Figure 4.20 shows the position of the vehicle throughout the main U-turn of DM2 while varying the maximum steering angle. The red dots represent 5 degrees, the yellow dots 10 degrees, the green dots 20 degrees, the pink dots 40 degrees and the dark blue dots 60 degrees.

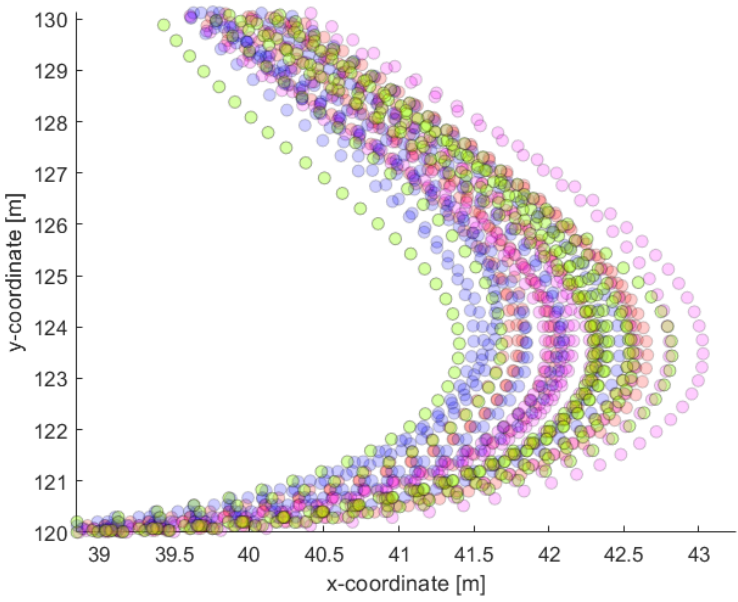

Figure 4.20: *Maximum steering angle variation for DM2.*

Generally, most of the results from varying the maximum steering angle fall into the interval of deviation because of non-determinism. Judging from the opacity of the dots, some trends can however be made out. It seems that the dots that represent the smaller steering angles, 5 and 10 degrees, seem to drift more outward during the turn, Meanwhile, the curve that represents the largest maximum steering angle, 60 degrees, seems to not drift as much.

4.4 Velocity profiles

The velocity profile using the default settings for DM2 is shown in Figure 4.21. In this case, the velocities were extracted directly from the ROS-topic publishing vehicle odometry, with the velocities expressed in (x,y).

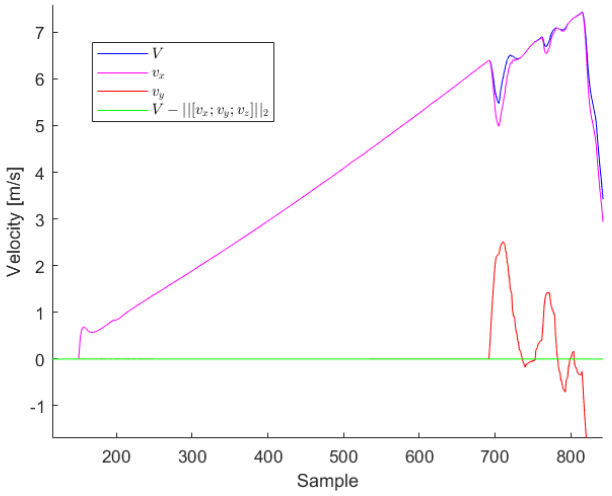

Figure 4.21: *Velocity profile for DM2, using vehicle odometry information.*

The figure shows the profiles for the total speed of the vehicle in the inertial coordinate system, the lateral and longitudinal velocities as well as the difference between the total speed and the 2-norm of the velocity vector. In the figure, it can be observed that the 2-norm of the velocities and the total velocity are identical throughout the entire course. The same variables are plotted in Figure 4.22.

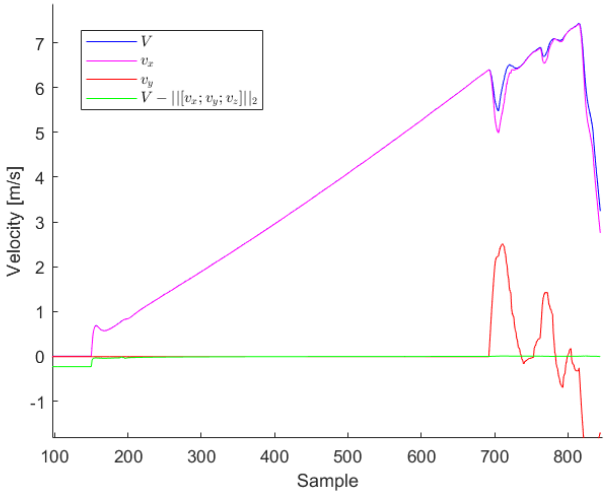

Figure 4.22: *Velocity profile for DM2, using vehicle status information.*

Here, the velocities are computed using the acceleration of the vehicle. The sampling frequency of the ROS-topics is 20 Hz. Here it can be seen that the difference between the total velocity and the 2-norm of the velocity vector seems to differ throughout the course, which can be seen more clearly in Figure 4.23.

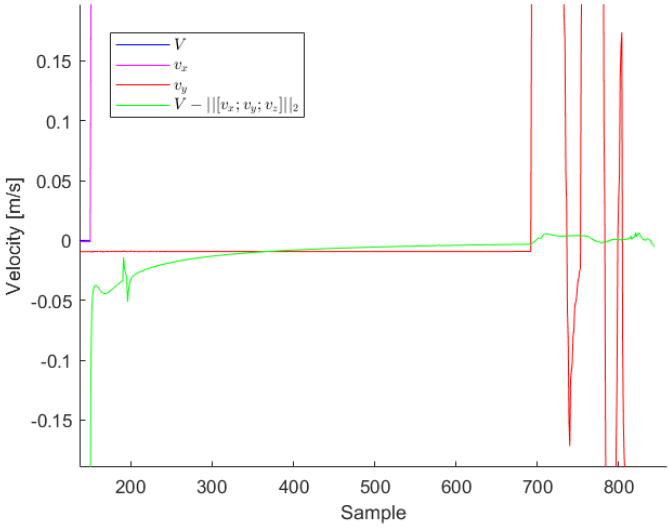

Figure 4.23: *Velocity profile for DM2, using vehicle status information. Zoomed in around x-axis.*

The difference between the speed of the vehicle and the norm was seen to increase for more extreme driving conditions, for example very low friction. At around sample 650 in the figures, there is a slight decrease in the total velocity and an increase in the lateral velocity. This is a result of the vehicle starting to turn but also an effect of the decrease in acceleration because of the Hybrid A* algorithm re-planning the path.

5

Discussion and conclusion

This chapter discusses the results and the trends that can be observed from the results. The determinism tests, parameter variations and smoothing options will be discussed and conclusions regarding these simulations and the results with respect to the problem formulation are presented.

5.1 Determinism of Hybrid A* and path following

This section provides a discussion about the results from the determinism tests, what causes this behaviour and how the parameter variations affect the deterministic behaviour of the vehicle.

5.1.1 Discussion of results from determinism test and sample frequency

It could be concluded from the determinism tests that the path planner seems to provide a deterministic solution when faced with a simple environment without any obstacles present. The vehicle control does not, however, give a deterministic behaviour, resulting in the vehicle taking different actions to reach the goal, with what seems to be at random. During the determinism tests, an increasing velocity did affect the severity of these non-deterministic effects. The path planning does not, however, seem to change in any way, which is reasonable since the reference velocity only is a parameter in the vehicle control and not a factor in the Hybrid A* algorithm.

What could be the causes of the non-deterministic behaviour? One possible cause was examined by measuring the sampling periods during a test run. It could be

seen that the sampling frequency of the ROS-bridge was mostly consistent with sampling at a rate of 10 Hz, while the controller was more inconsistent. Inconsistencies in sampling rate were both frequent and would vary between ≈ 6.7 Hz and 20 Hz. If the system at large runs with a sampling frequency of 10 Hz, but the controller at only ≈ 6.7 or 20 Hz on occasions, it is probably one source of the problem. If the entire system is not synchronized and the different sub-systems have different sampling rates, values used for computations can be changed in between sampling of the different systems and therefore result in unreliable results.

Apart from the problem with an inconsistent sampling rate throughout the system, it is out of the scope of the thesis project to investigate what could be causing this behaviour. It would of course be interesting to measure the sampling frequencies or all subsystems, but the source of error would likely not be found. Throughout the tests, it can be seen that the time it takes to initiate the program, plan the path and maximum velocities vary from run to run. This point towards uncertainties that seem to be dependent on both computational power at the time as well as the control of the vehicle from the PID controller.

5.1.2 Determinism when altering parameters and missions

Judging from the results from DM3, it can be concluded that the planned path is inconsistent when the vehicle is faced with an environment with obstacles and needs to re-plan during the mission. Since the vehicle control is not deterministic this is only reasonable, since the vehicle will likely never be at the same position with the same velocity and orientation twice. It will therefore be impossible to consistently give the Hybrid A* the same initial conditions in the middle of a mission and it will probably never come up with the exact same path. As defined in Chapter 3, determinism means producing the same outcome given that the initial conditions and parameters are the same. Hybrid A* is deterministic but will never be given the same initial conditions and parameters, resulting in that the total planned path is not consistent between each run.

For the first and second driving missions, the planned paths were generally consistent. The exception to this arose later in the missions, where the planner likely needed to make a new decision. The same problem then occurred as for DM3, and the planner was therefore unable to produce a consistent path for each run. This is as previously discussed caused by the non-determinism of the path following.

When varying the tire friction, there were generally no indications that a lower or higher friction would result in a more non-deterministic behaviour of the controller. The only test that somewhat stood out was the third test of DM1. During this test, it seemed that a higher friction resulted in a lower deviation between the runs, but since this trend only applies to this test case and there are uncertainties in the numerical estimation, no general conclusions can be drawn from this.

For DM1, there seems to be a correlation between a high vehicle mass and a

higher deviation between the runs. For DM2, the lowest deviation could be found for one of the lower vehicle masses, but no trend regarding the maximum deviation could be seen. It is uncertain if this depends on other factors or just on the uncertainty in the measurement of deviation. Since the trend for DM1 is so prominent it can, at least for lower velocities, be concluded that a very high vehicle mass seems to result in a larger deviation between the runs and therefore a larger uncertainty about the position of the vehicle during the driving mission.

Judging from DM2, there is a clear trend that an increase in reference velocity results in a larger deviation between the runs. This trend does, however, only seem to be present for the higher velocities. When varying the velocity between 1 and 5 m/s, no difference in the deviation between runs can be seen for these cases. It can be concluded that the velocity needs to be relatively high in order to affect the uncertainty in the position of the vehicle.

One other aspect to consider is the default run for the other parameter alterations, which used a reference velocity of 10 m/s but only managed to reach around 7 m/s. This provides an important clue of how a high velocity seems to affect the deviation significantly. For this default run on driving mission 2, the deviation seems to be around 1.5 m, the same value as for 10 m/s.

Since DM1 also introduced a variation of reference velocity, there are some observations from these tests as well. Generally, the third test seems to have the lowest values for the deviation compared to the first and second tests. The only variable changed from the first test to the third is the reference velocity, and it can therefore be concluded that a lower reference velocity for DM1 results in a smaller deviation between the runs and therefore less uncertainty about where the vehicle is. This case can also be compared with the results from DM2, which performed tests with the same reference velocities and identical maximum steering angle, with the only difference being the driving mission itself. The deviation of DM1 was lower than the corresponding test for DM2, which can only result in the conclusion that the deviation is dependent on the appearance of the route. A more aggressive turn will result in a larger uncertainty about the position of the vehicle.

Looking at DM2, there were no patterns regarding how the maximum steering angle affected the deviation. By comparing the first and second test of DM1, where the only difference was the maximum steering angle, no obvious trend could be seen regarding the deviation between runs. For some of the parameter variations, the increase of the maximum steering angle seemed to result in a larger deviation but for other variations it seems to have the opposite effect. No conclusion regarding how the maximum steering angle affects the uncertainty of the vehicle position can therefore be drawn.

5.2 Parameter variation

This section provides a discussion about how the variation of the vehicle parameters affected the vehicle behaviour for the different tests and driving missions. In order to draw any valuable conclusions from the results, the deviations from varying the parameter must be clearly greater than the deviations from the non-deterministic behaviour. Otherwise, it is impossible to determine whether a variation in position is because of a parameter alteration or simply because the system is non-deterministic.

5.2.1 Analysis of tire friction variation

The general trend when varying the tire friction is that a lower friction generally results in the vehicle drifting outwards in a turn. The vehicle is not affected greatly when the driving is not as extreme, which is why the foundation of the analysis is based on the behaviour when there is a need for steering. This is an important aspect of realistic driving, since the vehicle needs to be able to steer away from vehicles, pedestrians and other obstacles. If the drifting is too big, the vehicle behaviour is not reliable.

The cause of the drifting is that the vehicle control is not able to follow the path planned by Hybrid A* because of the road surface being very slippery. Neither the vehicle control or Hybrid A* takes the tire-road interaction into account, which mean that the problem lies with both the path planning and the path following. The Hybrid A* planner provides the vehicle control with a set of waypoints which, given the constraints of the kinematic single-track model, should be feasible for the vehicle to reach. The vehicle control is tasked with computing the desired speed and steering angles to reach these waypoints, but since there are effects present that make the kinematic single-track model not applicable, the planned route is no longer drivable and the vehicle control will not be able to follow the intended path. Regardless if the tire friction is 50μ or 0.05μ, the steering commands will be identical but the outcome will be completely different when the tire friction is very low. The vehicle will drift and the controller will work to compensate for the error in speed and steering angle, but it has been shown in the results that the controller is unable to solve the problem with a non-drivable planned path.

The vehicle side slip angle of the vehicle was heavily dependent on the tire friction. For the first test of DM1, very low friction resulted in a vehicle side slip angle of approximately 6 degrees and an increase of the tire friction quickly increased the vehicle side slip angle as well. For the lowest frictions, 0.05μ and 0.1μ, the decrease in vehicle side slip angle was prominent. There were, however, no large changes in vehicle side slip angle when varying the friction between 0.5μ and 50μ. The same trend applies to the other tests of DM1 and DM2 as well. For all frictions of 0.5μ and above, the vehicle side slip angle remains constant at around 20 degrees for DM1 and around 25 degrees for DM2.

The rear tire side slip angle was generally small for all tests where the tire friction

was varied. There is no clear trend visible throughout all tests, but one interesting result is that for the friction 0.1μ for DM2, where the vehicle drifted too much to get any decent comparisons to the other parameter values. The side slip angle of the rear tire increased dramatically compared to when using the friction 0.3μ. The huge side slip angle corresponds to the vehicle drifting heavily, which correlates to the observed behavior. It does, however, seem like the side slip angle for the rear tire is consistently around 5 degrees for all other settings. This can be considered small, which is one assumption for the validity of the dynamic single-track model. The assumption for the kinematic single-track model only holds when the vehicle is driving straight, which is where both the vehicle side slip angle and rear tire side slip angle are zero.

The yaw rate of the vehicle during the turn is also dependent on the tire friction. A lower friction was also observed to result in a lower yaw rate of the vehicle and as for the vehicle slip angles, this value remains constant for all frictions above 0.5μ. The yaw angle and vehicle side slip angle both seem to relate to how well the vehicle can maneuver through the course. A lower yaw angle does indicate that the vehicle is unable to steer as desired, which can be connected to a low friction, as described in Section 3.3.

Judging from how the position of the vehicle varied when the friction parameter was altered, the lower friction choices seemed to result in the vehicle drifting further from the intended path. This is not consistent with the value of the vehicle side slip angle, which indicates that a lower friction seems to result in a vehicle that slides less laterally than when using a higher friction. One explanation for this, which also correlates with the low yaw rate, is that the vehicle as a result of the low friction surface is unable to rotate and thus drifts mostly longitudinally.

DM3 was different from the previous missions in the sense that the vehicle was given the opportunity to find its own way through the course. It was clear that the lowest friction, 0.1μ, resulted in the vehicle not staying on the planned route and drifting around the course. Apart from this observation, no other trends could be extracted from the test, since it is impossible to know if the behaviour is because of the planned path being different or the parameter variations. This applies both when varying the tire friction and the vehicle mass.

For all the driving missions and test cases, it was seen that the friction needed to be lowered very much in order to see the effects that can be expected from a low friction. Increasing the friction did not seem to have any noticeable effects on the turn-taking of the vehicle, other than possibly increasing the steepness of the turn slightly. The Hybrid A* planner does seem to be robust against most variations in friction, but sensitive to extremely low friction values.

Hybrid A* fails to take the tire-road interaction into account, since it only uses the kinematic single-track model for describing the vehicle behaviour. If a dynamic model was instead used for determining the possible motion primitives, the tire-road interaction and therefore also the lateral dynamics could be taken into account to compute a more realistic solution. In real-life applications, such

low frictions that are simulated here are rarely observed and it can therefore generally be concluded that the Hybrid A* algorithm is robust against changes in tire friction.

5.2.2 Analysis of vehicle mass variation

When varying the vehicle mass, the effects on the vehicle position were not as prominent as for the tire friction variations. In both DM1 and DM2, it was not possible to differentiate the effects of varying the vehicle mass and non-determinism from just observing the vehicle positions.

It was not possible to observe any correlations between the vehicle mass and the vehicle side slip angle. For DM2, the yaw rate decreased with increasing vehicle mass. This could be related to that a heavy vehicle can not reasonably turn as fast as a light vehicle. This does not seem to have any effect on the vehicle side slip angle, however. The rear tire side slip angles were generally small. The trend that could be observed was that a lighter vehicle did seem to generate a larger rear tire side slip angle. Looking at the dynamic single-track model in Equation (2.6), a smaller vehicle mass results in a larger lateral acceleration and hence also a larger lateral velocity and side slip angle which is consistent with the obtained results. Based on the model in the physics engine described by Equation (2.1), the velocity will increase with a decreasing vehicle mass. Assuming the velocity increases for a lighter vehicle, the yaw rate will also increase, judging from Equation 2.5.

5.2.3 Analysis of reference velocity variation

The first and third tests of DM1 investigated how the variation of velocity in combination with the variation of friction or vehicle mass affects the vehicle behaviour. When varying the friction parameter, the effects of lowering the friction seemed to be more prominent when the reference velocity was set as 5 m/s than for 3 m/s. For the reference velocity 3 m/s, it could only be concluded that the lowest friction setting, 0.05μ, did result in the vehicle drifting outwards in the curve. Using reference velocity 5 m/s, the same effect could be seen for both 0.05μ and 0.1μ. The vehicle seems to be more sensitive to changes in friction when the velocity is higher.

The hypothesis can be confirmed by looking at DM2. The reference velocity is set to 10 m/s but the vehicle only reaches a top speed of around 7 m/s. As discussed, the effects of lowering the friction during DM2 are big and results in the vehicle drifting far from the path. As described in Chapter 3, the friction 0.05μ was not possible to use in the simulations due to the vehicle drifting so far from the course. It is difficult to determine if the driving mission or the increased velocity is the biggest reason for this. It is probably a combination of the two. There does, however, seem to exist a correlation between the velocity and the sensitivity to friction variations.

The results from DM1 point towards the vehicle side slip angle increasing and the yaw rates decreasing with a decreasing velocity. The decreasing yaw rates were

very prominent both when varying friction and vehicle mass. This trend was also present in DM2. A high velocity does heavily increase the yaw rate of the vehicle during the turn. As described in Equation (2.5), the yaw rate depends on the total velocity of the vehicle, which explain why a higher velocity can result in a higher yaw rate. When reaching a reference velocity of approximately 10 m/s, the increase in yaw rate seems to stagnate, since the yaw rate of 10 m/s and 15 m/s is nearly identical. This is likely owing to limitations on the rotation of the vehicle since it regardless of the velocity needs to adhere to the laws of physics.

The side slip angle at the rear tire shows the same trend as for the vehicle side slip angle during DM1, where a lower velocity results in a larger side slip angle. The trend is somewhat different during DM2. Both the largest and lowest velocities do in this case result in large side slip angles. The large side slip angle for low velocities can be explained by the limitation in yaw rate, where the same reasoning applies to the vehicle side slip angle. As described in Chapter 3, the side slip angle of the rear tire is dependent on the dimensions, yaw rate as well as the lateral and longitudinal velocity of the vehicle. A very low yaw rate will have a huge impact on the lateral dynamics of the vehicle, and therefore also on the slip. The behaviour of the side slip angle when driving at 15 m/s is deviant from the results of the vehicle side slip angle. For this velocity, where the vehicle was observed to deviate greatly from the intended path, the side slip angle increased compared to when driving at 10 m/s. When driving at 10 m/s, the vehicle does seem to be able to compensate for the effects caused by the large velocity with a large yaw rate and therefore avoid drifting and leaving the planned path. When the velocity increases, the yaw rate is approximately the same as for 10 m/s, but the effects of the increasing velocity are greater and the vehicle is therefore not able to compensate, resulting in drifting from the intended path.

When varying the reference velocity, an increase from 1 m/s to 3 m/s and up to 5 m/s results in a slightly different behaviour of the vehicle during the turn of DM2. The routes are somewhat similar and but it is still clear that an increase in velocity affect the vehicle position. Increasing the reference velocity over 5 m/s has much larger effects of the position. For 10 m/s and 15 m/s, the vehicle heavily deviates from the intended path. It can therefore be concluded that the reference velocity has big effects on the vehicle behaviour. For the larger velocities the vehicle is not able to steer onto the desired path in time, even though the yaw rate of the vehicle is much higher than for the lower velocities.

5.2.4 Analysis of maximum steering angle variation

When the friction parameter was varied during DM1, no changes could be seen between test 1 and 2 where the single difference was the value of the maximum steering angle. The vehicle side slip angles, side slip angles of the rear tire and yaw rates were identical throughout these tests, with the uncertainty of numerical estimations of the values probably being the only source of error. When varying the vehicle mass, one trend arose during test 2 of DM1, where the heavier vehicle configuration resulted in steeper turn-taking. This trend was not present for

the first test, and is therefore likely a result of increasing the maximum steering angle. During DM2, the side slip angle at the rear tire seemed to decrease slightly when the maximum steering angle of 60 degrees was chosen. With a larger maximum steering angle, the vehicle has access to a wider control set, which gives the vehicle control a better possibility of following the planned path. The Hybrid A* planner does have a separate control set defined and plan the path based on that the maximum steering angle of the vehicle is $2\pi/3$ rad, which is approximately 39 degrees.

The same trend can be seen for DM2. It was concluded that the test with the largest maximum steering angle, 60 degrees, resulted in the vehicle taking a more direct path towards the next waypoint. A larger steering angle gives the vehicle more maneuverability, which will help the vehicle stay on the path especially during steep turns. A large maximum steering angle allows the vehicle to better compensate for any disturbances that occur and at the same time decreasing the rear tire side slip angle. Decreasing the maximum allowed steering angle, which does impact the vehicle control directly, resulted in the vehicle not being able to follow the intended path as directly as when a large maximum steering angle was used. This is solely because of the limitations put on the vehicle control and does not concern the limitations of the Hybrid A* planner at all.

5.2.5 Validity of velocity measurements

From Figure 4.21, it can be seen that the velocities extracted from the vehicle odometry seem to be accurate. Since the difference between the total velocity and the norm of the velocity vector is zero throughout the entire course, this means that the extracted longitudinal and lateral velocities are correct in comparison to the total velocity. In Figure 4.22, this difference was not zero all the time, which indicates that there are some inaccuracies in the computation of the velocities. This could be because of the inconsistent sampling frequencies mentioned earlier where it was concluded that the system work at a sample rate of approximately 10 Hz, but this rate deviates between ≈ 6.7 and 20 Hz for the PID controller.

When using the acceleration of the vehicle to compute the velocity, which uses a sampling rate of 20 Hz, compared to the sampling rate of the system, which is 10 Hz, the velocity computation is exposed to errors. This mismatch of sampling rates is most likely the cause of the velocities computed from the accelerations not corresponding to the real velocity of the vehicle. This is therefore not a good method to use when dealing with inconsistent sampling rates.

5.3 Smoothing functions

Varying the chord length between 1.5 and 4.8 m did not have a significant impact on the appearance of the planned route. When the chord length increases to 6 m, the appearance of the planned route changes along with how well the vehicle follows the route. This is of course heavily dependent on the look-ahead parameter

as well. There is no answer to what the optimal chord length is, since it is dependent on the application. If the intention is to follow the planned path as closely as possible, the chord length 3.3 m seems to generally be the best. During the first curve, the chord length 6 m is the best for representing the real behaviour of the vehicle. For the other configurations, the real path deviates from the planned path during this turn. In order to get the smoothest path possible, the best option would be a higher value of the chord length.

As stated in Chapter 4, some interesting results were obtained around the position (100,0) as shown in Figure 4.9. There are multiple planned waypoints within a few meters of this coordinate, which should be impossible given the nature of the Hybrid A* algorithm. The first goal state is placed at position (100,0) which means that Hybrid A* needs to plan a new route when reaching this point. When the vehicle is within the goal radius of (100,0), the next goal state is set as (150,-50) and a new path has to be planned while the vehicle is still moving. The re-planning and the fact that the vehicle is moving while the path is planned, meaning that the initial state of the vehicle according to the planner does not correspond to the actual position of the vehicle for long, is likely the cause of the inconsistencies of the path around (100,0). This applies mainly to the default setting.

The most important aspect when discussing the look-ahead parameter is the balance between a smooth, and perhaps more realistic path, and a path that resembles the Hybrid A* solution. As for the chord length variation, the answer to what the best choice is depends entirely on the goal. A low look-ahead results in the vehicle following a very smooth and straight path whereas a higher value more closely follows the planned path produced by Hybrid A*.

By looking at the results from the parameter variations, one important question is if a change in look-ahead could possibly dampen the effects from for example a very low friction. It has been concluded that a very low friction results in the vehicle drifting heavily especially during steep turns. With the use of the look-ahead parameter, the planned path could be smoothed out and therefore making the effects of the lower friction smaller. The problem with the vehicle deviating from the indented path will still remain, but using this as a tool for the cases where the drifting is the worst could be an option.

5.4 Conclusions

Hybrid A* is deterministic but the planned path is not identical throughout the simulation, since the non-determinism of the path following fails to provide Hybrid A* with the same initial conditions every execution. It is more likely to get a consistent path when the mission is short and free of obstacles. It can be concluded that a very large vehicle mass and high velocities result in a larger uncertainty regarding the position of the vehicle. A more aggressive turn does also increase the non-deterministic behaviour of the path planner. No conclusions regarding the impact of the tire friction or maximum steering angle on the

deterministic behaviour could be made.

The Hybrid A* algorithm is robust against changes in vehicle mass. There is no need to know the vehicle mass exactly, the vehicle will behave roughly identical regardless of the mass, ranging between 100 to 10000 kg.

The algorithm is not robust against extremely low tire friction. When considering somewhat normal road conditions, the friction will not affect the behaviour in any considerable way and the Hybrid A* solution will be valid and robust against friction variations. If the tire friction is extremely low, the fact that Hybrid A* currently does not take tire-road interaction into account when planning the path is very limiting and results in that the solution provided by the path planner does not reflect realistic driving behaviour.

Lowering the maximum steering angle enough will make the vehicle unable to follow the solution provided by the Hybrid A* algorithm. Since Hybrid A* plans the path based on the motion primitives, which in turn is based on a set of possible steering angles, a disconnection between the planner and the allowed steering commands from the PID-controller will result in the vehicle not being able to follow the planned path. In conclusion, it is important that the maximum steering angle of the PID controller corresponds with the constraints used by the Hybrid A* algorithm.

The vehicle behaviour is highly sensitive to changes in reference velocity and an increase in velocity does make the vehicle deviate from the path planned by Hybrid A*. The fact that the kinematic single-track model does not take the velocity of the vehicle and the constraints on how fast the vehicle can turn into consideration is the main limitation of the Hybrid A* planner. When driving at larger velocities, there is a need for dynamics and the kinematic single-track model is not sufficient for those cases.

The chord length and look-ahead parameter could be utilized for the cases where the deviation between the planned and real path is greatest in order to create a smoother path. This could possibly make the real path better correspond to the path provided by Hybrid A*.

Based on the assumptions for the vehicle models and tire models, nothing can be said about the slip angles at the front tire because of the problem with obtaining the steering angles. The side slip angles at the rear tire are generally small with the exception of very low frictions as well as very high and low velocities. The vehicle side slip angles are generally very high, but the analysis show that the obtained velocities that are used for calculating all side slip angles are valid.

By looking at the assumptions of the vehicle models described in Chapter 2 and the obtained results, the kinematic model should theoretically be valid only for non-extreme driving with mostly light turns and when the vehicle is driving straight. The assumptions for the dynamic single-track model hold for most cases except for extreme velocities and very low friction.

It is once again important to differentiate the general Hybrid A* algorithm from

the implementation of the Hybrid A* algorithm. In reality, the current implementation of the Hybrid A* algorithm seems to be able to compute a drivable and realistic path for all cases except the most extreme parameter choices. The algorithm is therefore concluded to be robust for variation in vehicle mass, tire friction and maximum steering angles but very sensitive to a change in velocity, given the current implementation of the path planner and path following. The kinematic single-track model does therefore seem to mostly be limited to high velocities but is still an acceptable model for small slip angles. The dynamic single-track model is better suited for larger velocities, since it models the dynamics and the tire forces. The motion equations used in the physics engine use the same principle as the dynamic single-track model and are therefore also well suited to handle these driving missions.

The usage of the kinematic single-track model in the Hybrid A* algorithm can be concluded to be sufficient in describing the vehicle behaviour in most cases. The dynamic single-track model is more suitable for higher velocities, but the choice of vehicle model is not critical in all other cases. A low degree of accuracy in regards to the dynamics of the vehicle is needed, since the Hybrid A* planner is able to compute a realistic and drivable path despite not taking the dynamics of the system into consideration. Complete knowledge of the dynamics of the vehicle is not needed in order to achieve a good enough representation of its behaviour, with the exception of higher driving velocities, where a dynamic model is needed.

5.5 Future work

This section describes the continuation and other possible topics that relate to this thesis project. Some applications that were not possible to explore because of limitations and other factors are discussed further.

In order to provide a deeper understanding of the system and the non-determinism exhibited by the vehicle, it would be interesting to collect more data and study how for example the distribution of position looks when increasing the number of sample runs drastically. The number of runs tested in this thesis project does not provide a good statistical base, the number of runs needs to be much higher in order to draw any conclusions regarding the distributions. If the problem of time synchronization could somehow be solved, knowledge about the vehicle behaviour could be increased by studying the nature of the distributions more closely.

Many of the papers presented in Section 1.5 utilized a MPC controller, since the vehicle modeling can be integrated to the controller itself. This has proved to be successful and would be an interesting continuation of this thesis project. It would be interesting to explore how the effects discovered through his project would be affected by using the MPC controller instead, and explore the limitations of the PID controller further.

The thesis project only covered the aspect of altering parameters in order to get a smoother path. The usage of a smoothing function is possible but the implementation of this was beyond the scope of this thesis project. A future possibility would be to investigate how a smoothed Hybrid A* solution would affect the vehicle behaviour and make comparisons with the results obtained in this thesis project.

Since the modification of the vehicle and tire models was deemed too complicated to be within the scope of this thesis project, a future possibility would of course be to work on this further. The models are defined in the physics engine and a more software-oriented thesis project would be more suitable in order to define new and alter the old models.

One extension to the thesis project is to use the knowledge of how the vehicle behaves based on different road surfaces and velocity profiles. Since it could be concluded that an increased velocity makes the vehicle more sensitive towards low friction surfaces, limitations on the vehicle speed dependent on the current velocity could be implemented. Modeling the risk of drifting out of course dependent on the velocity and friction and determining the maximum allowed velocity based on this would be a possible solution. Assuming an autonomous vehicle that can detect for example ice patches on the road during a sharp turn, the reference velocity could be lowered in order to minimize drifting and possibly also accidents.

The thesis only considered single parameter alterations in order to minimize the complexity and easily find the cause of a certain behaviour. One future possibility is to extend the scope to also include multiple parameter variations in order to investigate how the parameters interact with and affect each other.

Appendix

A

Complete testing results

This chapter provides the detailed results regarding the slip angles, yaw rates and deviation between runs for DM1 and DM2. Since the detailed results from DM3 were irrelevant in the analysis of the parameter variations, the results from this driving mission are not presented.

Table A.1: *Detailed results for Driving mission 1, Test 1*

DM1 - Test1, $v = 5$ **m/s,** $\delta = 10$ **m/s**					
Friction [factor of μ**]**	β [deg]	α_r [deg]	$\dot{\psi}$ [deg]	Maximum velocity [m/s]	Deviation between runs [m]
0.05	5.9	6.5	20	4.96	1.5-2
0.1	12.1	-3.3	30	5.04	1-1.5
0.5	17.8	-5.3	44	4.96	0.5-1
1	18.9	-5.5	45	5.00	1
1.5	18.6	-5.5	46	5.01	1
10	18.5	-5.5	46	4.99	1-1.5
50	18.8	-5.5	45	4.98	0.5-1

Mass [kg]	β [deg]	α_r [deg]	$\dot{\psi}$ [deg]	Maximum velocity [m/s]	Deviation between runs [m]
100	19.5	-6.5	47	4.98	0.5-1
500	18.5	-6	44	4.95	1
1000	18.6	-5.5	45	4.99	1
1500	18.9	-5.5	45	5.00	1
2000	18.5	-5.5	45	4.99	1
4000	18.5	-5.5	46	4.95	1
10000	18	-5	46	4.94	1-2

Table A.2: *Detailed results for Driving mission 1, Test 2*

DM1 - Test2, $v = 5$ **m/s,** $\delta = 20$ **m/s**					
Friction [factor of μ**]**	β [deg]	α_r [deg]	$\dot{\psi}$ [deg]	Maximum velocity [m/s]	Deviation between runs [m]
0.05	6	6.5	20	4.97	1
0.1	12	-3.2	31	5.05	1
0.5	18.5	-5.5	45	4.97	0.5-1
1	18.5	-5.5	45	4.98	1
1.5	19	-5.7	45	4.97	1-1.5
10	18.5	-5.5	44	4.97	1
50	18	-5.3	44	4.97	1

Mass [kg]	β [deg]	α_r [deg]	$\dot{\psi}$ [deg]	Maximum velocity [m/s]	Deviation between runs [m]
100	19	-6	47	4.99	1
500	18.5	-5.5	45	4.97	1
1000	18.5	-5.3	44	4.98	1
1500	18.5	-5.5	45	4.98	1
2000	18.5	-5.5	45	5.00	1
4000	18	-5.5	44	4.96	1
10000	18	-5.5	46	4.94	1-1.5

Table A.3: *Detailed results for Driving mission 1, Test 3*

DM1 - Test3, $v = 3$ **m/s,** $\delta = 10$ **m/s**					
Friction [factor of μ**]**	β [deg]	α_r [deg]	$\dot{\psi}$ [deg]	Maximum velocity [m/s]	Deviation between runs [m]
0.05	15	-5	-20	3.04	0.5
0.1	18	-6.3	-24	3.03	0.2
0.5	20	-7	-25	3.01	0.5
1	20	-7	-26	3.03	0.5
1.5	20	-7	-26	3.01	0.2
10	20	-7.2	-25	3.01	0.5
50	20	-7.2	-27	3.01	1

Mass [kg]	β [deg]	α_r [deg]	$\dot{\psi}$ [deg]	Maximum velocity [m/s]	Deviation between runs [m]
100	20	7	-28	3.00	0.5
500	20	-6.7	-26	3.01	0.5
1000	20	-6.7	-26	3.01	0.5
1500	20	-7	-26	3.03	0.5
2000	20	-6.7	-27	3.03	0.5
4000	20	-7	-26	3.02	0.5
10000	20	-6.7	-28	3.05	1

Table A.4: *Detailed results for Driving mission 2*

DM2					
Friction [factor of μ]	β [deg]	α_r [deg]	$\dot{\psi}$ [deg]	Maximum velocity [m/s]	Deviation between runs [m]
0.3	-22	5.5	75	7.21	1
0.5	-25	6	85	7.17	1
1	-25	7	90	7.20	1.5
1.5	-26	7.5	90	7.17	1
10	-26	7	90	7.31	0.5
50	-26	7.3	90	7.32	1.5

Mass [kg]	β [deg]	α_r [deg]	$\dot{\psi}$ [deg]	Maximum velocity [m/s]	Deviation between runs [m]
100	-26	8.5	93	7.18	1.5-2
500	-24	5.5	90	7.31	0.5
1000	-25	6	92	7.42	1
1500	-25	7	90	7.20	1.5-2
2000	-26	7	90	7.17	1.5
4000	-26	7	87	7.18	1
10000	-26	7	85	7.02	1

Reference velocity [m/s]	β [deg]	α_r [deg]	$\dot{\psi}$ [deg]	Maximum velocity [m/s]	Deviation between runs [m]
1	-34	14	15	1.04	1
3	-32	12	35	2.99	1
5	-30	10.5	65	4.85	1
10	-25	-5.5	120	9,1	1.5
15	-16	-11	124	14.3	3

Max steer angle [deg]	β [deg]	α_r [deg]	$\dot{\psi}$ [deg]	Velocity	Deviation between runs [m]
5	-26	7	87	7.3	1
10	-25	7	90	7.20	1.5
20	-26	7	87	7.4	1.5
40	-26	7	87	7.4	1
60	-25	6	90	7.5	1

Bibliography

[1] J. Petereit, T. Emter, C. W. Frey, T. Kopfstedt, and A. Beutel, "Application of Hybrid A* to an Autonomous Mobile Robot for Path Planning in Unstructured Outdoor Environments," in *ROBOTIK 2012; 7th German Conference on Robotics*, pp. 1–6, 2012.

[2] "CARLA Documentation." `https://carla.readthedocs.io/en/latest/`. Accessed: 2022-01-31.

[3] "ROS Documentation." `http://wiki.ros.org/Documentation`. Accessed: 2022-01-31.

[4] "ROS Bridge Documentation." `https://carla.readthedocs.io/projects/ros-bridge/en/latest/`. Accessed: 2022-01-31.

[5] J. de Winter, P. Leeuwen, and R. Happee, "Advantages and Disadvantages of Driving Simulators: A Discussion," 2012.

[6] A. A. Ahmed, J. Santhosh, and F. W. Aldbea, "Vehicle Dynamics Modeling and Simulation with Control Using Single Track Model," in *2020 IEEE International Women in Engineering (WIE) Conference on Electrical and Computer Engineering (WIECON-ECE)*, pp. 1–4, 2020.

[7] D. Dolgov, S. Thrun, M. Montemerlo, and J. Diebel, "Practical Search Techniques in Path Planning for Autonomous Driving," *AAAI Workshop - Technical Report*, 01 2008.

[8] D. Dolgov, S. Thrun, M. Montemerlo, and J. Diebel, "Path Planning for Autonomous Vehicles in Unknown Semi-structured Environments," *The International Journal of Robotics Research*, vol. 29, pp. 485–501, 2010.

[9] B. Paden, M. Čáp, S. Z. Yong, D. Yershov, and E. Frazzoli, "A Survey of Motion Planning and Control Techniques for Self-Driving Urban Vehicles," *IEEE Transactions on Intelligent Vehicles*, vol. 1, no. 1, pp. 33–55, 2016.

[10] F. Gao, Q. Hu, J. Ma, and X. Han, "A Simplified Vehicle Dynamics Model for Motion Planner Designed by Nonlinear Model Predictive Control," *Applied Sciences*, vol. 11, no. 21, pp. 1–18, 2021.

[11] T. Tiwari, S. Agarwal, and A. Etar, "Controller Design for Autonomous Vehicle," in *2021 International Conference on Advances in Electrical, Computing, Communication and Sustainable Technologies (ICAECT)*, pp. 1–5, 2021.

[12] P. Polack, F. Altché, B. d'Andréa Novel, and A. de La Fortelle, "The kinematic bicycle model: A consistent model for planning feasible trajectories for autonomous vehicles?," in *2017 IEEE Intelligent Vehicles Symposium (IV)*, pp. 812–818, 2017.

[13] R. Rajamani, *Vehicle Dynamics and Control*. Springer New York Dordrecht Heidelberg London, second ed., 2012.

[14] J. Wong, *Theory of Ground Vehicles*. John Wiley Sons, Inc., third ed., 2001.

[15] J. Kong, M. Pfeiffer, G. Schildbach, and F. Borrelli, "Kinematic and dynamic vehicle models for autonomous driving control design," in *2015 IEEE Intelligent Vehicles Symposium (IV)*, pp. 1094–1099, 2015.

[16] H. B. Pacejka, *Tire and Vehicle Dynamics*. Butterworth-Heinemann, second ed., 2051.

[17] L. Hao, L. Guo, and S. Liu, "Vehicle Running State Estimation by Adaptive Soft-Sensing Algorithm," *Mathematical Problems in Engineering*, vol. 2018, no. 2, p. 9, 2018.

[18] A. Gasparetto, P. Boscariol, A. Lanzutti, and R. Vidoni, "Path Planning and Trajectory Planning Algorithms: A General Overview," *Mechanisms and Machine Science*, vol. 29, pp. 3–27, 03 2015.

[19] A. Elfes, "Using occupancy grids for mobile robot perception and navigation," *Computer*, vol. 22, no. 6, pp. 46–57, 1989.

[20] P. E. Hart, N. J. Nilsson, and B. Raphael, "A Formal Basis for the Heuristic Determination of Minimum Cost Paths," *IEEE Transactions on Systems Science and Cybernetics*, vol. 4, no. 2, pp. 100–107, 1968.

[21] S. Sedighi, D.-V. Nguyen, and K.-D. Kuhnert, "Guided Hybrid A-star Path Planning Algorithm for Valet Parking Applications," in *2019 5th International Conference on Control, Automation and Robotics (ICCAR)*, pp. 570–575, 2019.

[22] T. Glad and L. Ljung, *Reglerteknik-Grundläggande teori*. Studentlitteratur AB, fourth ed., 2014.

[23] P. Renard, A. Alcolea, and D. Ginsbourger, "Stochastic versus Deterministic Approaches," in *John Wainwright, Mark Mulligan (Eds), Environmental Modelling: Finding Simplicity in Complexity*, vol. 1, pp. 133–149, 2013.

[24] S. Grollius, M. Ligges, J. Ruskowski, and A. Grabmaier, "Concept of an Automotive LiDAR Target Simulator for Direct Time-of-Flight LiDAR," *IEEE Transactions on Intelligent Vehicles*, pp. 1–1, 2021.